AD-A136 574   MATHEMATICAL MODELS FOR DAMAGEABLE STRUCTURES(U) NEW   1/1
               MEXICO UNIV ALBUQUERQUE BUREAU OF ENGINEERING RESEARCH
               M L WANG ET AL. MAR 83 CE-64(83)AFOSR-993-1
UNCLASSIFIED   AFOSR-TR-83-1256 AFOSR-81-0086   F/G 12/1   NL

END
FILMED
1-84
DTIC

MICROCOPY RESOLUTION TEST CHART

NATIONAL BUREAU OF STANDARDS-1963-A

②

A136574

THE UNIVERSITY OF NEW MEXICO
COLLEGE OF ENGINEERING

BUREAU OF ENGINEERING RESEARCH

MATHEMATICAL MODELS FOR DAMAGEABLE STRUCTURES

by

Ming-Liang Wang

Thomas L. Paez

Frederick Ju

Technical Report CE-64(83)AFOSR-993-1

March 1983

DTIC
ELECTE
JAN 5 1984
D

84 01 04 042

REPORT DOCUMENTATION PAGE	READ INSTRUCTIONS BEFORE COMPLETING FORM
1. REPORT NUMBER AFOSR-TR- 83-1256 2. GOVT ACCESSION NO. AD-A136574	3. RECIPIENT'S CATALOG NUMBER
4. TITLE (and Subtitle) MATHEMATICAL MODELS FOR DAMAGEABLE STRUCTURES	5. TYPE OF REPORT & PERIOD COVERED INTERIM
	6. PERFORMING ORG. REPORT NUMBER
7. AUTHOR(s) MING-LIANG WANG THOMAS L. PAEZ FREDERICK JU	8. CONTRACT OR GRANT NUMBER(s) AFOSR-81-0086
9. PERFORMING ORGANIZATION NAME AND ADDRESS UNIVERSITY OF NEW MEXICO BUREAU OF ENGINEERING RESEARCH ALBUQUERQUE, NM 87131	10. PROGRAM ELEMENT, PROJECT, TASK AREA & WORK UNIT NUMBERS 61102F 2307/C2
11. CONTROLLING OFFICE NAME AND ADDRESS AIR FORCE OFFICE OF SCIENTIFIC RESEARCH/NA BOLLING AFB, DC 20332	12. REPORT DATE March 1983
	13. NUMBER OF PAGES 88
14. MONITORING AGENCY NAME & ADDRESS(if different from Controlling Office)	15. SECURITY CLASS. (of this report) Unclassified
	15a. DECLASSIFICATION/DOWNGRADING SCHEDULE

16. DISTRIBUTION STATEMENT (of this Report)

Approved for Public Release; Distribution Unlimited.

Accession For
NTIS GRA&I ☑
DTIC TAB ☐
Unannounced ☐
Justification

By
Distribution/
Availability Codes
Dist | Avail and/or Special
A-1

17. DISTRIBUTION STATEMENT (of the abstract entered in Block 20, if different from Report)

18. SUPPLEMENTARY NOTES

19. KEY WORDS (Continue on reverse side if necessary and identify by block number)

shock	equivalent linear systems	high order linear systems
vibration	time varying linear systems	damage
blast	energy dissipation	
inelastic structures	peak response	

20. ABSTRACT (Continue on reverse side if necessary and identify by block number)

The reliability of a structural system at a particular time depends on the damage level in the system. When the damage level exceeds a critical value, then failure occurs. Therefore, it is important to track the damage in a structure. In the present investigation some basic models are proposed for the study of damageable structure response. The models are: (1) a higher order linear differential equation with constant coefficients, and (2) a second order linear differential equation with time varying coefficients. Using a digital computer, a blast input is simulated, and the response of an inelastic

DD FORM 1473 EDITION OF 1 NOV 65 IS OBSOLETE
1 JAN 73

MATHEMATICAL MODELS FOR DAMAGEABLE STRUCTURES

by

Ming-Liang Wang

Thomas L. Paez

Frederick Ju

The University of New Mexico

(Department of Civil Engineering
and
Department of Mechanical Engineering

March 1983

ACKNOWLEDGEMENT

ABSTRACT

The reliability of a structural system at a particular time depends on the damage level in the system. When the damage level exceeds a critical value, then failure occurs. Therefore, it is important to track the damage in a structure. In the present investigation some basic models are proposed for the study of damageable structure response. The models are: (1) a higher order linear differential equation with constant coefficients, and (2) a second order linear differential equation with time varying coefficients. Using a digital computer a blast is simulated, and the response of an inelastic structure is computed. Noise signals are added to these and the results are used to simulate measured input and response. Next, using the simulated input and response, the parameters of the linear models are identified and the linear structure responses are computed. Measures of these responses, incuding peak displacement and energy dissipated are compared to the simulated response. It is shown that the models accurately simulate inelastic structure response. Moreover, the results of some experiments are included. The experiments show that the energy dissipated in a material specimen is related to the damage level.

TABLE OF CONTENTS

LIST OF FIGURES

LIST OF TABLES

CHAPTER 1

1.0 Introduction

When a structure is excited by an external force, it executes a response determined by the characteristics of both the input and the structure. We could predict the exact response of a structure, characterized by its geometry and its mutual properties, if we could predict inputs exactly; if we had a perfect model for the structure; and if our mathematical computations were correct. However, since inputs are random, we cannot perfectly characterize complex structures, and since mathematical models are not perfect, we can only estimate the response of a structure.

In structural analysis we wish to assess the response of a structure to dynamic loads, such as blasts and earthquakes. This procedure, of course, requires the use of a dynamic model which will permit us to predict the response of a structure accurately. These structural models are generally chosen to fit experimental data and to simplify mathematical computations.

Most existing structures were designed based on a static model, and although dynamic properties may be considered in their design, the designed parameters may be inadequate to predict the response to dynamic load correctly. Considerable work has been performed on identifying the parameters of mathematical models from dynamic experimental data, and various approaches have been proposed for predicting system parameters based on experimental data.

These identified parameters can be used to predict the dynamic response of a structure to a different excitation than that used to test it. The identified parameters also can be used to calculate the energy dissipation in a hysteretic structure caused by strong excitation.

The energy dissipated by a structure during a strong motion response is an indication of the structural damage. It is important to predict how much damage occurs in a structure due to strong motion because the level of damage is related to the likelihood of structural failure. When damage does occur, it can appear in different forms, such as cracks, permanent deformation, or change in characteristic frequency.

While damage may be located through visual inspection, such an inspection may not accurately estimate either its magnitude or exact location. Consequently, it is difficult to assess whether the structure would survive normal design conditions or another severe excitation. By visual inspection, it may be possible to locate the damage area. When damage occurs it is desirable to estimate its magnitude and locate it, if possible.

1.1 Literature Review

Part of the energy dissipated by a structure is dissipated due to hysteretic behavior of the structural material. The equation governing the hysteretic response of a lumped mass system is a second-order, nonlinear, ordinary differential equation with history-dependent stiffness term. Two models which may approximate the nonlinear system will be proposed in this report. These are:

1. High-order equivalent linear system;
2. Time-varying parameter linear system.

The first model considered in this paper is a high-order equivalent linear system. It is assumed that the nonlinear hysteretic system is approximately governed by a high-order equivalent system. This model is motivated by studies summarized in the literature. For example, Lutes and Hseih [1] used a third-order linear system to approximate a single-degree-of-freedom (SDF) oscillator with bilinear hysteretic yielding behavior, excited by stationary white noise. In the linear system, certain

2

parameters were chosen so that the rms displacement and velocity matched empirical values for the nonlinear system. They showed that the third-order system gives a better overall prediction of response buildup than does either the linear SDF system or a two-mode system.

Lutes [2] used a different type of equivalent linear system to approximate the nonlinear system. All the methods Lutes considered defined the equivalence either in terms of response displacement level, velocity level, frequency, or a combination of these. He found that a particular equivalent linear system can generally only be expected to match a limited number of response statistics of a particular nonlinear system with a particular type of excitation.

Wen [3], and Wen and Baber [5, 6] have used the equivalent linearization method to approximately represent the response of a hysteretic SDF system. They showed that the third order, linear, differential equation provided a satisfactory representation of the inelastic, hysteretic systems. This closed form linearization is relatively simple to formulate which allows ready extension to multi-degree-of-freedom (MDF) systems. They showed that the equivalent linearization method gives satisfactory results at all response levels for response analysis of MDF deteriorating or non-deteriorating systems under random excitation.

Another study by Wafa [7] demonstrated that the peak response for an hysteretic SDF system excited by random inputs is closely predicted by a third order, linear, equivalent system. Recent work [8] has also shown that the high-order linear equivalent model provides a good approximation to the hysteretic system when the energy dissipated and frequency shift are concerns. Significantly, the results established that the parameters of a higher order system can be identified by using a frequency domain method even when noise is present both in the forcing and response signals. In contrast, the time domain approach yields

3

poor results in the presence of noise. Because of the frequency domain's preferable application, it will be used to do the analysis.

The second model is motivated by the fact that structures may exhibit time-variant nonlinear response to strong motion. This implies that structure deterioration was in progress during the large amplitude motion. Such a phenomenon has been recognized and studied in the past. For example, Udwadia and Trifunac [9] and Iemura and Jennings [10] carried out an analysis to characterize such behavior in terms of a quasi-time-variant linear formulation based on the data obtained from the San Fernando earthquake of February 9, 1971.

In another study Townsend and Hanson [11] demonstrate time-varying hysteretic loops by the experimental test of reinforced concrete beam-column and T-shaped specimens under different loading conditions. In addition, Uzumeri [12] has also shown the same behavior for an experimental study of cast-in-place reinforced concrete beam-column joints subjected to simulated seismic loading.

Based on the above referenced investigations involving time-varying parameters system, we anticipate that the time-varying parameter model will provide a good representation of a hysteretic system.

1.2 Objective

The determination of the system parameters from suitable experimental observations is a fundamental problem in engineering. Obtaining a good representation of a system requires all the proper information, such as well measured data and a suitable model.

The objective of this study is to justify two possible models to characterize the behavior of a system. The relative merits of each model are discussed. Extensive numerical experimentation using simulated data is also presented in order to investigate their feasibility and accuracy. This study will demonstrate how well the system parameters can be identified with and without noise in the measurements. Once the parameters are known, the energy dissipated by the system can be computed. Based on the computed results, one can compare how well the models performed for a given set of data. The ultimate goal of this study is to establish structural models useful for other purposes, such as prediction, design, control, and damage assessment.

The present research has been aimed at the analysis of damage accumulation in concrete structures. It is assumed that when a concrete structure dissipates energy, it accumulates damage. To justify this assumption some physical experiments have been performed. Specifically, concrete cylinders have been subjected to cyclic loading. The energy dissipated in each cylinder was measured and the level of residual strength in each cylinder was determined after the load cycling was completed. The residual strength was plotted versus energy dissipated. When the reduction in strength is taken as a measure of damage, this plot reveals the damage caused by energy dissipation.

CHAPTER 2
HIGH ORDER EQUIVALENT LINEARIZATION

2.1 Model

The differential equation governing the response of a
single-degree-of-freedom (SDF) system is

$$m\ddot{z} + u = f \tag{2-1}$$

where m is the mass of the structure, f is the forcing function,
z is the displacement response, dots denote differentiation with
respect to time, and u is the restoring force of the structure.
Equation (2-1) can be used to model the actual system in which u
can be a very complicated function. In the present study, the
hysteretic restoring force, u, is modeled by using the equation

$$\sum_{j=0}^{M} c_j u^{(j)} = c_{M+1}\dot{z} + z \tag{2-2}$$

where the c_j, j = 0, 1, ..., M+1 are the constants governing
the system restoring force characteristics, where $u^{(j)}$ denotes
the jth time derivative of u, and M is a constant denoting the
order of approximation provided by the linear system. The reason
for using this model to represent the hysteretics system is that
it displays a hysteretic character that can be made to match the
character of an inelastic structure.

Consider the case where M is equal to 0. The model in Equa-
tions 2.1 and 2.2 becomes

$$m\ddot{z} + \frac{c_1}{c_0}\dot{z} + \frac{1}{c_0}z = f \tag{2-3}$$

6

$$0.259\ddot{z} + 7.77\dot{z} + 5829z$$
$$= 300 \, e^{-10t} \sin 150t$$
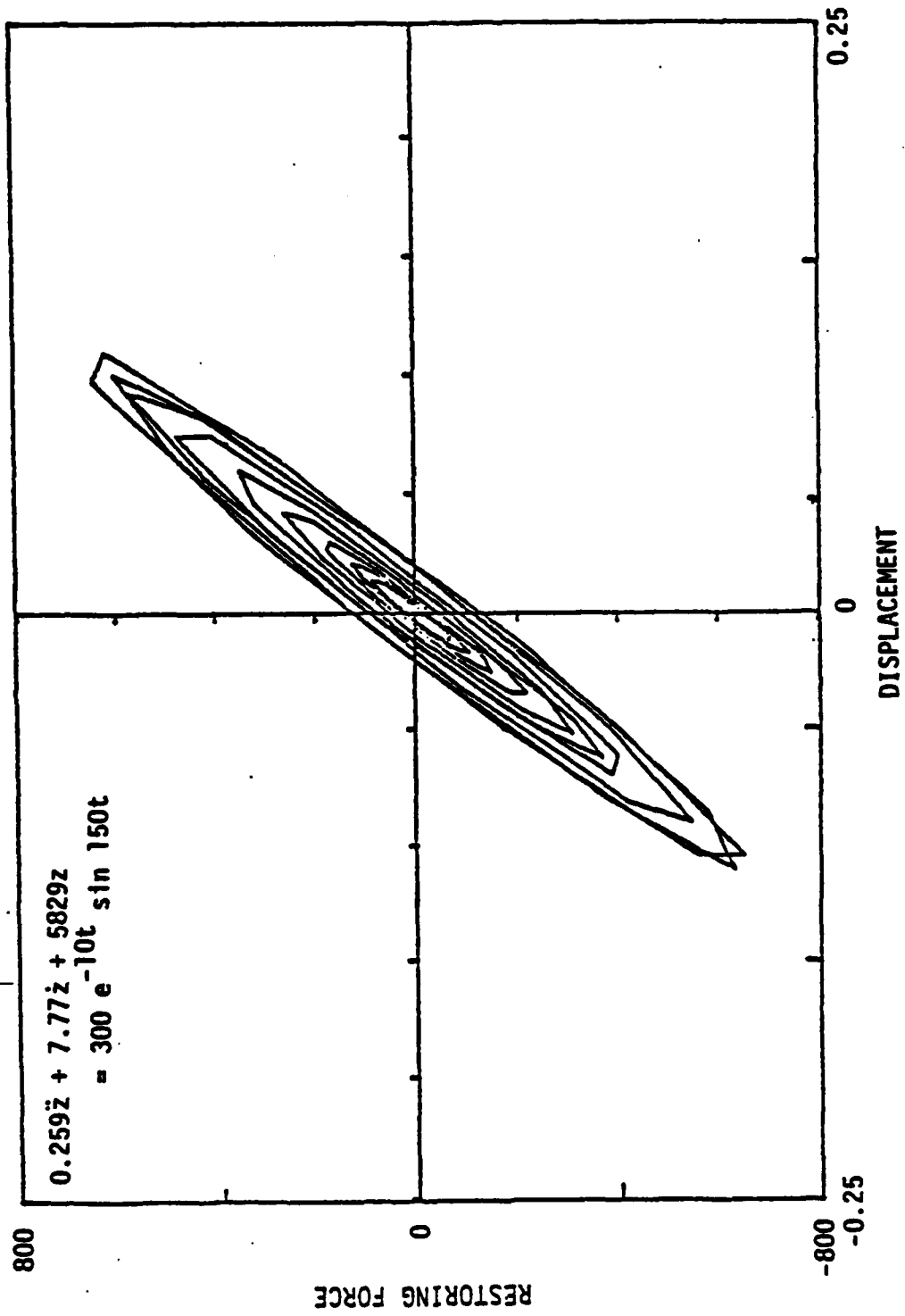
Figure 2.1 Total restoring force versus displacement for second-order system

7

$$0.259\ddot{z} + u = 300\ e^{-10t}\ \cos 150t$$
$$3.96 \times 10^{-4}\ u + 6.25 \times 10^{-6}\ \dot{u}$$
$$= 3.94 \times 10^{-2}\dot{z} + z$$

DISPLACEMENT
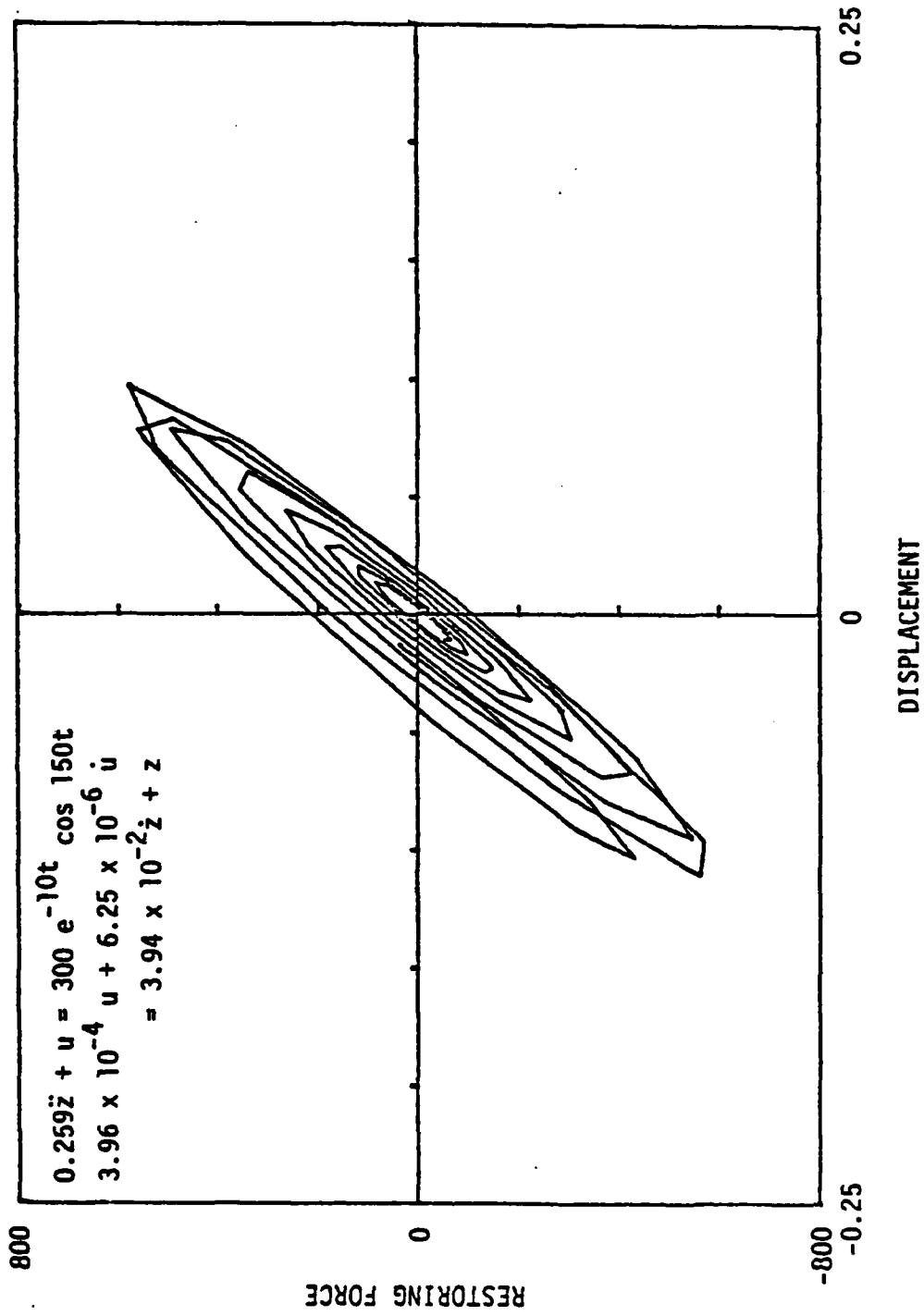
RESTORING FORCE

Figure 2.2   Total restoring force versus displacement for third-order system

8

This is simply the second-order linear differential equation governing the SDF system. However, when the response of the actual system is linear and damping is viscous, the model of Equation (2-3) represents the actual system. The restoring force function for this system is $u = (c_1/c_0)z + (1/c_0)z$. This model displays the hysteretic behavior as shown in Figure (2.1).

When the constant M is chosen as 1 in equation 2-2, the model becomes

$$m\ddot{z} + u = f$$
$$c_0 u + c_1 \dot{u} = c_2 \dot{z} + z \tag{2-4}$$

Combining these equations results in

$$\frac{c_1}{c_0} m\ddot{z}' + m\ddot{z} + \frac{c_2}{c_0}\dot{z} + \frac{1}{c_0}z = f + \frac{c_1}{c_0}\dot{f} \tag{2-5}$$

The parameters of the system in Equation (2-5) can be chosen so that the model represents the hysteretic system as well as possible.

For example, Figure (2.2) shows the hysteretic properties for an SDF system by plotting the restoring force versus displacement. The parameters for the system and the forcing input are given in Figures (2.2). This study will consider both the equations (2-3) and (2-5).

The parameters can be identified by using the least-square identification criterion. Since most observed data include a certain percentage of noise, the frequency domain approach will be used to perform the parameter identification. However, a practical problem of accuracy arises in the parameter identification problem for high-order linear systems. Therefore, the

high-order systems, for $M > 1$, will not be considered in the following discussion. It is anticipated that in some cases, the third-order linear approximation (Equation 2-5) provides a better representation of the hysteretic system than the second-order linear system (Equation 2-3).

2.2 Identification of Parameters

The problem of parameter identification can be posed as one class in the broader topic of optimization. The object of parameter identification is to make inferences about the real world and mathematical models on the basis of measured input data. The measured data in this study were assumed available, and were simulated to represent the field data.

First, it is assumed that there is no noise present in the measured data. Then, noise data are introduced. Note that the measured response data are given as acceleration values. This is realistic since the structural response acceleration is often the measured quantity in an experimental test.

2.2a Second Order System

Now, consider the second-order model, Equation 2-3, Equation 2-3 can be simplified by taking

$$\frac{1}{c_0} = a_0, \quad a_1 = \frac{c_1}{c_0} \tag{2-6}$$

The equation governing motion of the system becomes

$$m\ddot{z} + a_1\dot{z} + a_0 z = f \tag{2-7}$$

Fourier transform both sides to obtain

$$m(i\omega)^2 Z(\omega) + a_1(i\omega)Z(\omega) + a_0 Z(\omega) = F(\omega) \tag{2-8}$$

where

10

$$Z(\omega) = \int_{-\infty}^{\infty} z(t)\ e^{-i\omega t}\ dt \quad -\infty < \omega < \infty$$

$$F(\omega) = \int_{-\infty}^{\infty} f(t)\ e^{-i\omega t}\ dt \quad -\infty < \omega < \infty \tag{2-9}$$

are the Fourier transforms of $z(t)$ and $f(t)$, respectively. This equation can be rearranged and combined with $Z(\omega)$ and $F(\omega)$ terms on one side of the equation to obtain

$$(-m\omega^2 + a_0 + a_1 i\omega) = \frac{F}{Z} \tag{2-10}$$

Multiply each side of the equation by its complex conjugate to obtain the modulus squared.

$$\left| -m\omega^2 + a_0 + a_1\ i\omega \right|^2 = \frac{|F|^2}{|Z|^2} \tag{2-11}$$

Evaluate the left side and let $|F|^2 \big/ |Z|^2$ equal $Q(\omega)$ to obtain

$$\left(a_0 - m\omega^2 \right)^2 + (a_1\omega)^2 = Q(\omega) \tag{2-12}$$

This equation can be used to identify the parameters of second-order linear system. However, this equation is exactly satisfied if and only if: 1) the system under consideration is linear; 2) all measurements are noise free; and, 3) the Fourier transforms of $\ddot{z}(t)$ and $f(t)$ used in Equation (2-12) are exact. When these requirements are not satisfied, Equation 2-12 will include an error term (or noise term). This practical case is usually the one that needs the most attention.

When noise is present on the measured input and response, Equation 2.12 can be written as

$$\left(a_0 - m\omega^2 \right)^2 + (a_1\omega)^2 = Q(\omega) + \varepsilon(\omega) \tag{2-13}$$

11

Note from Equation 2-7 that a_0 is the equivalent stiffness and a_1 is the equivalent damping for the second-order linear system. Therefore, a_0 is greater in magnitude than a_1. In view of this and the form of Equation 2-13, a_0 can be estimated by noting the frequency where $Q(\omega) + \varepsilon(\omega)$ is a minimum whenever the equivalent damping factor is much less than 1 (say less than 0.2). This will be true in most civil engineering systems.

Denote the frequency where $Q(\omega) + \varepsilon(\omega)$ is a minimum by ω_m. Equation 2-13 shows that, approximately,

$$a_0 = m\omega_m^2 \qquad\qquad (2\text{-}14)$$

since the first term on the left is approximately zero when $Q(\omega) + \varepsilon(\omega)$ is a minimum. Substitute Equation 2-14 into Equation 2-13; this yields

$$m^2(\omega_m^2 - \omega^2) + (a_1\omega)^2 = Q(\omega) + \varepsilon(\omega) \qquad\qquad (2\text{-}15)$$

Now, it is necessary to find the coefficient a_1 which minimizes the $\varepsilon(\omega)$.

The coefficients a_1 can be evaluated using a least-squares approach, where the integral of $\varepsilon^2(\omega)$ over a specific range of frequencies is minimized. Based on Equation 2-15, set

$$\int_{\omega_a}^{\omega_b} \left(a_1^2\omega^2 + m^2(\omega_m^2 - \omega^2) - Q(\omega)\right)^2 d\omega = \varepsilon^2(\omega) \qquad (2\text{-}16)$$

where ω_a amd ω_b are lower and upper bound frequencies, respectively. This frequency band is chosen so that the system response behavior can be fully characterized. It is anticipated

that the frequency band includes the natural frequency for a linear or slightly non-linear system. For a highly nonlinear system, the characteristic frequency, ω_m, will shift. However, the frequency band can be located by finding the frequency where $Q(\omega) + \epsilon(w)$ is a minimum, and selecting the frequency band around this frequency.

In general, the lower frequency, ω_a, is located at a point where its corresponding $Q(\omega_a) + \epsilon(\omega_a)$ value is about 5 times as great as the minimum value of $Q(\omega) + \epsilon(\omega)$; and ω_b is the higher frequency where $Q(\omega_b) + \epsilon(\omega_b)$ is about 5 times greater than the minimum value of $Q(\omega) + \epsilon(\omega)$. This method is used to select ω_a and ω_b based on an approximate linear analysis. When ω_a and ω_b are chosen in this manner, the interval (ω_a, ω_b) will be approximately the half power bandwidth of the system. This frequency interval reflects the characteristics of the system.

Take the first partial derivative of ϵ^2 with respect to $a_1{}^2$, and set it equal to 0. The result is

$$\frac{\partial \epsilon^2}{\partial a_1{}^2} = 2 \int_{\omega_a}^{\omega_b} \left(a_1{}^2 \omega^2 + m^2 (\omega_m{}^2 - \omega^2)^2 - Q(\omega) \right) \omega^2 \, d\omega = 0 \quad (2\text{-}17)$$

Simplify this to obtain

$$a_1{}^2 \int_{\omega_b}^{\omega_a} \omega^4 \, d\omega = \int_{\omega_a}^{\omega_b} \left(Q(\omega) - m^2 (\omega_m{}^2 - \omega^2)^2 \right) \omega^2 \, d\omega \quad (2\text{-}17a)$$

Integrate the equation where possible to get

13

$$a_1^2 = \frac{5}{\omega_b^5 - \omega_a^5}\left\{\int_{\omega_a}^{\omega_b} \omega^2\, Q(\omega)\, d\omega - m^2\left[\frac{\omega_m^4}{3}(\omega_b^3 - \omega_a^3)\right.\right.$$

$$\left.\left. - \frac{2}{5}\,\omega_m^5(\omega_b^5 - \omega_a^5) + \frac{1}{7}(\omega_b^7 - \omega_a^7)\right]\right\} \tag{2-18}$$

Let $\omega_a = q_a\,\omega_m$ $\qquad\qquad\qquad\qquad\qquad\qquad$ (2-19)

$\qquad\ \omega_b = q_b\,\omega_m$

where q_a is a coefficient less than one and q_b is a coefficient greater than one. This equation can be further simplified

$$a_1^2 = \frac{\omega_m^2}{q_b^5 - q_a^5}\left\{\frac{5}{\omega_m^7}\int_{\omega_a}^{\omega_b}\omega^2\, Q(\omega)\, d\omega + m^2\left[-\frac{5}{3}(q_b^3 - q_a^3)\right.\right.$$

$$\left.\left. + 2(q_b^5 - q_a^5) - \frac{5}{7}(q_b^7 - q_a^7)\right]\right\} \tag{2-20}$$

This equation provides the value of a_1. This is the best estimator in the least-squares sense. All the parameters in this equation are known except the integral of the $\omega^2 Q(\omega)$ term which can be evaluated numerically.

2.2b Third Order Equation

The second-order linear ordinary differential equation may not be considered an accurate representation of the hysteretic system. It is hoped that the third-order linear system may improve the accuracy in some sense.

Equation 2-5 can be simplified by taking

$$\frac{1}{c_0} = a_0, \qquad \frac{c_2}{c_0} = a_1, \qquad \frac{c_1}{c_0} = a_2 \tag{2-21}$$

14

Then Equation 2-5 becomes

$$ma_2 \, \dddot{z} + m\ddot{z} + a_1\dot{z} + a_0 z = f + a_2\dot{f} \tag{2-22}$$

Fourier transform both sides to get

$$\frac{\left(ma_2 \, (i\omega)^3 + m(i\omega)^2 + a_1 \, (i\omega) + a_0\right)}{\left(1 + a_2 \, (i\omega)\right)} = \frac{F}{Z} \tag{2-23}$$

The symbols used in this equation have the same meaning as in earlier equations. Multiply each side of the equation by its complex conjugate to yield the modulus squared

$$\frac{\left| - ima_2\omega^3 - m\omega^2 + ia_1\omega + a_2 \right|^2}{\left| 1 + ia_2 \, \omega \right|^2} = \frac{|F|^2}{|Z|^2} \tag{2-24}$$

Evaluate the left hand side and let $|F|^2\big/|Z|^2$ be replaced by $Q(\omega)$ to obtain

$$\frac{(a_0 - m\omega^2)^2 + \omega^2 \, (a_1 - m\omega^2 a_2)^2}{1 + (a_2\omega)^2} = Q \, (\omega) \tag{2-25}$$

This equation governs a third-order linear system in the frequency domain. Measured data can satisfy this equation exactly if and only if: 1) the system under consideration is linear; 2) all measurements are noise free; and, 3) the Fourier transforms used to define $Q(\omega)$ are exact. These conditions, however, are not usually met. In fact, the purpose of this investigation is to use the higher-order linear system to represent an hysteretic system. Therefore, measured data do not usually satisfy the

15

above equation. To account for this explicitly, Equation 2-25 is written

$$\frac{(a_0 - m\omega^2)^2 + \omega^2(a_1 - m\omega^2 a_2)^2}{1 + (a_2\omega)^2} = Q(\omega) + \varepsilon(\omega) \qquad (2\text{-}26)$$

$\varepsilon(\omega)$ is a noise term which must be minimized by the proper choice of system parameters. This equation can be used to identify the system parameters following several approaches. Two of these are summarized below. One approach approximates certain terms in Equation 2-25 to obtain estimates for the system parameters, while the other approach uses a search technique to estimate system parameters.

The first method to be investigated is an approximate technique. When a_2 is small compared to the characteristic frequency, ω_m of an SDF system, the $(a_2\omega)^2$ term in the denominator can be neglected. This is usually true when nonlinear deformation is not too large. Eliminate the $(a_2\omega)^2$ term in Equation 2-26 to obtain

$$(a_0 - m\omega^2)^2 + \omega^2 (a_1 - m\omega^2 a_2)^2 = Q(\omega) + \varepsilon(\omega) \qquad (2\text{-}27)$$

When a_1 and a_2 are small compared to a_0 (which is usually the case, the minimum of the left-hand side occurs near the frequency

$$\omega = \sqrt{\frac{a_0}{m}} \qquad (2\text{-}28)$$

As previously described, the characteristic frequency, ω_m, can be found when the $Q(\omega) + \varepsilon(\omega)$ term is a minimum. In terms of ω_m, a_0 can be written

$$a_0 = m\omega_m^2 \qquad (2\text{-}29)$$

16

Expand the second term on the left side of Equation 2-27 and use the result of Equation 2-29. Neglect the $m^2\omega^4 a_2^2$ term. Then Equation 2-27 becomes

$$m^2 (\omega_m^2 - \omega_k^2)^2 + \omega^2 (a_1^2 - 2m\omega^2 a_1 a_2) = Q(\omega) + \epsilon(\omega) \quad (2\text{-}30)$$

Let $a_1^2 = b_1$ and $a_1 a_2 = b_2$, then $\qquad\qquad\qquad\qquad (2\text{-}31)$

$$\omega^2 (b_1 - 2m\omega^2 b_2) - \left(Q(\omega) - m^2(\omega_m^2 - \omega^2)^2 \right) = \epsilon(\omega) \qquad (2\text{-}32)$$

When this expression is evaluated at the discrete frequency

$\omega = \omega_k$, the result is

$$\omega_k^2 (b_1 - 2m\omega_k^2 b_2) - \left(Q_k - m^2(\omega_m^2 - \omega_k^2)^2 \right) = \epsilon_k \qquad (2\text{-}33)$$

The system parameters, a_1 and a_2, can now be identified as those which minimize the sum of the squares of the ϵ_k terms in Equation 2-33. Consider a sequence of discrete frequencies uniformly spaced in the interval (ω_a, ω_b). These are ω_a, $\omega_a + \Delta\omega$, $\omega_a + 2\Delta\omega$, etc. Define

$$\{b\} = (b_1 \quad b_2)^T \qquad\qquad\qquad\qquad (2\text{-}34a)$$

$$[x_1] = \begin{bmatrix} \omega_a & -2m\omega_a^4 \\ \omega_a + \Delta\omega & -2m(\omega_a + \Delta\omega)^4 \\ \omega_a + 2\Delta\omega & -2m(\omega_a + 2\Delta\omega)^4 \\ \cdot & \cdot \\ \cdot & \cdot \\ \cdot & \cdot \\ \omega_b & -2m\omega_b^4 \end{bmatrix} \qquad (2\text{-}34b)$$

17

$$\{x_2\} = \begin{Bmatrix} Q_{\omega_a} & - m^2\left(\quad (\omega_m{}^2 - \omega_a{}^2)\right)^2 \\ Q_{\omega_a + \Delta\omega} & - m^2\left(\omega_m - (\omega_a + \Delta\omega)^2\right)^2 \\ Q_{\omega_a + 2\Delta\omega} & - m^2\left(\omega_m{}^2 - (\omega_a + 2\Delta\omega)^2\right)^2 \\ \vdots & \vdots \\ Q_{\omega_b} & - m^2(\omega_m{}^2 - \omega_b{}^2)^2 \end{Bmatrix} \qquad (2\text{-}34c)$$

$$\{\varepsilon\} = (\varepsilon_{\omega_a} \quad \varepsilon_{\omega_a + \Delta\omega} \cdots \varepsilon_{\omega_b}) \qquad (2\text{-}34d)$$

Note $\Delta\omega$ is equal to $(2\pi/T)$ and T is the total duration of the excitation. (ω_a, ω_b) defines the range of frequencies over which the system is analyzed. As in the identification of parameters of the second-order linear system, only a portion of the frequency range is used in the parameter identification.

This frequency range can be chosen as before. In terms of the matrices defined above, Equation 2-32 can be written at discrete frequencies as

$$[x_1] \{b\} - \{x_2\} = \{\varepsilon\} \qquad (2\text{-}35)$$

The vector $\{b\}$ can be found by minimizing the sum of the squares of $\{\varepsilon\}$. This is $\varepsilon^2 = \{\varepsilon\}^T \{\varepsilon\}$. The vector $\{b\}$ which minimizes ε^2 is

$$\{b\} = ([x_1]^T[x_1])^{-1}[x_1]^T \{x_2\} \qquad (2\text{-}36)$$

When b_1 and b_2 have been computed, a_1 and a_2 can be found from Equation 2-31.

$$a_1 = \sqrt{b_1}, \quad a_2 = b_2/a_1 \qquad (2\text{-}37)$$

18

This solution provides approximate values for the parameters in the third-order linear system which represents the hysteretic system.

Another approach can be used for the estimation of parameters in the higher order linear system. This is a search procedure which iteratively estimates the parameter values. Equation 2-26 can be rewritten

$$\epsilon(\omega) = Q(\omega) - \frac{(a_0 - m\omega^2)^2 + \omega^2 (a_1 - m\omega a_2)^2}{1 + (a_2\omega)^2} \qquad (2\text{-}38)$$

This quantity is a measure of the mismatch between the measured data, reflected in $Q(\omega)$, and the model, reflected in the second term on the right side of Equation 2-38.

This mismatch can be either positive or negative and can be used to define one measure of the difference between the model and the measured data over a range of frequencies. This measure is

$$\epsilon^2 = \sum_k \epsilon(\omega_k) \qquad (2\text{-}39)$$

where the sum is taken over those discrete frequencies in the interval (ω_a, ω_b). This is the square error of the model. This error is minimized, however, when the model parameters are chosen to satisfy the sequence of equations

$$\frac{\partial \epsilon^2}{\partial a_0} = 0 = \frac{\partial \epsilon^2}{\partial a_1} = \frac{\partial \epsilon^2}{\partial a_2} \qquad (2\text{-}40)$$

The parameters a_0, a_1, and a_2, which satisfy these equations establish a model which is optimal in a least squares sense.

Equations 2-40 can be solved numerically using a search technique. A computer program was written to solve Equation

19

2-40. The program, included in the appendix, uses Newton's method to search for the solution. The analysis procedure followed in the computer program is identical to that used in solution of the problem summarized in the following section. The steps in the solution procedure are listed at the end of Chapter 3.

CHAPTER 3

SYSTEM WITH TIME-VARYING PARAMETERS

3.0 Time-Varying Parameters Model

Sructures may exhibit time-variant nonlinear response to
strong motion excitation. Time-varying structural properties
were not considered in the previous chapters. In this chapter, a
structure is modeled as a time variant single-degree-of-freedom
(SDF) oscillator, and a methodology is introduced to determine
its parameters using the observed data. It is important to
introduce a technique which can be applied when noise is present
in the measured data.

To demonstrate this procedure, consider an SDF linear system
with mass m. Let the damping and stiffness parameters for this
system be time varying. Its equation of motion is

$$m\ddot{z} + C(t)\dot{z} + K(t)\, z = f \tag{3-1}$$

in which z is the displacement response of the system; $C(t)$ and
$K(t)$ are time variant damping and stiffness function of the sys-
tem, respectively; and f is the forcing funtion. It is proposed
that this equation be used to model the behavior of a system
governed by Equation 2-1. Observe the system from time 0 to T
and assume that $z(0) = 0$ and $\dot{z}(0) = 0$.

The functions ($C(t)$ and $K(t)$ are assumed to have the form

$$C(t) = (1 + \alpha t)\, c_0$$

$$K(t) = (1 + \beta t)\, k_0 \tag{3-2}$$

Here, c_0 and k_0 are the damping constant and the stiffness con-
stant, respectively. α and β are consant coefficients which are
usually much less than one.

21

In many practical cases, it is observed that the structure displays an increase in damping and a decrease in stiffness when the structure excites an inelastic response. This implies α is a positive constant and β is a negative constant.

In this study, although α and β will be considered as small values, they will be large enough to influence the system's properties. This permits treatment of Equation 3-1 as a perturbed differential equation. When α and β are both equal to 0 (unperturbed), the equation 3-1 is simply a second-order differential equation with constant coefficients which can be easily solved.

The solution of Equation 3-1 can be written in the form (for example reference 18)

$$z = z_0 + \alpha z_\alpha + \beta z_\beta + \text{high-order terms} \tag{3-3}$$

Since α and β are small, the high-order terms will be neglected. Substituting Equation 3-3 into 3-1 and expanding yields

$$m(\ddot{z}_0 + \alpha\ddot{z}_\alpha + \beta\ddot{z}_\beta) + c_0 (1 + \alpha t) (\dot{z}_0 + \alpha\dot{z}_\alpha + \beta\dot{z}_\beta)$$
$$+ k_0 (1 + \beta t) (z_0 + \alpha z_\alpha + \beta z_\beta) = f \tag{3-4}$$

Moving the force term to the left side of the equation, grouping coefficients of the terms, 1, α, and β, then equating the coefficients to zero results in

$$m\ddot{z}_0 + c_0\dot{z}_0 + k_0 z_0 = f \tag{3-5a}$$

$$m\ddot{z}_\alpha + c_0\dot{z}_\alpha + k_0 z_\alpha = - c_0 t \dot{z}_0 \tag{3-5b}$$

$$m\ddot{z}\beta + c_0\dot{z}\beta + k_0 z_\beta = - k_0 t z_0 \tag{3-5c}$$

These equations approximately govern the system's response when time variation of the parameters is linear, as shown in Equation

3-2. If the excitation and the system's response are known, then
these equations can be used with a time domain parameter
identification procedure to estimate the system parameters.
However, when a time-domain parameter identification approach is
used, problems arise if noise is present in the measured input
and response signals (see Reference 8).

A frequency domain approach to the identification of system
parameters is pursued. Therefore, the equations of motion are
transformed to the frequency domain.

Let

$$Z_0(\omega) = \int_{-\infty}^{\infty} z_0(t) \ e^{-i\omega t} \ dt \qquad (3\text{-}6a)$$

$$Z_\alpha(\omega) = \int_{-\infty}^{\infty} z_\alpha(t) \ e^{-i\omega t} \ dt \qquad (3\text{-}6b)$$

$$Z_\beta(\omega) = \int_{-\infty}^{\infty} z_\beta(t) \ e^{-i\omega t} \ dt \qquad (3\text{-}6c)$$

define the Fourier transforms of $z_0(t)$, $z_\alpha(t)$, and $z_\beta(t)$.
And let

$$z_0(t) = \frac{1}{2\pi} \int_{-\infty}^{\infty} Z_0(\omega) \ e^{i\omega t} \ d\omega \qquad (3\text{-}7a)$$

$$z_\alpha(t) = \frac{1}{2\pi} \int_{-\infty}^{\infty} Z_\alpha(\omega) \ e^{i\omega t} \ d\omega \qquad (3\text{-}7b)$$

$$z_\beta(t) = \frac{1}{2\pi} \int_{-\infty}^{\infty} Z_\beta(\omega) \ e^{i\omega t} \ d\omega \qquad (3\text{-}7c)$$

define the inverse Fourier transforms. Then the Fourier transform of Equation 3-3 is

$$Z(\omega) = Z_0 + \alpha Z_\alpha + \beta Z_\beta \qquad (3-8)$$

It can be shown that the Fourier transform of Equations 3-5a through 3-5c are given by

$$-m\omega^2 Z_0(\omega) + c_0 \, i\omega Z_0(\omega) + k_0 \, Z_0(\omega) = F(\omega) \qquad (3-9a)$$

$$-m\omega^2 Z_\alpha(\omega) + c_0 \, i\omega Z_\alpha(\omega) + k_0 Z_\alpha(\omega) = c_0\Big(Z_0(\omega) + \omega Z'_0(\omega)\Big) \qquad (3-9b)$$

$$-m\omega^2 Z_\beta(\omega) + c_0 \, i\omega Z_\beta(\omega) + k_0 Z_\beta(\omega) = -i \, k_0 \, Z'_0(\omega) \qquad (3-9c)$$

Now solve the Equations 3-9 simultaneously. The result is

$$Z_0(\omega) = H(\omega) \, F(\omega) \qquad (3-10a)$$

$$Z_\alpha(\omega) = c_0 H(\omega) \Big(H(\omega)F(\omega) + \omega\big(H'(\omega)F(\omega) + H(\omega)F'(\omega)\big)\Big) \qquad (3-10b)$$

$$Z_\beta(\omega) = -ik_0 H(\omega) \Big(H'F(\omega) + H(\omega) \, F'(\omega)\Big) \qquad (3-10c)$$

where $H(\omega)$ is frequency response function and $H'(\omega)$ is its first derivative. These can be written in the forms

$$H(\omega) = [(k_0 - m\omega^2) + i(\omega c_0)]^{-1} \qquad (3-11a)$$

$$H'(\omega) = (2m\omega - ic_0) \, [(k_0 - m\omega^2) + i(\omega c_0)]^{-2} \qquad (3-11b)$$

$F(\omega)$ is the Fourier transform of $f(t)$ and $F'(\omega)$ is its derivative.

$$F(\omega) = \int_{-\infty}^{\infty} f(t) \, e^{-i\omega t} \, dt \qquad (3-12a)$$

24

$$F'(\omega) = -i \int_{-\infty}^{\infty} tf(t) \, e^{-i\omega t} \, dt \qquad\qquad (3\text{-}12b)$$

Substitute the results from Equations 3-10 into Equation 3-8. This yields

$$Z(\omega) = H(\omega)F(\omega) + \alpha c_0 \, H(\omega)\Big(H(\omega)F(\omega) + \omega(H'(\omega)F(\omega)$$
$$+ H(\omega)F'(\omega)\Big) + (-ik_0\beta) \, H(\omega)\Big(H'(\omega)F(\omega) + H(\omega)F'(\omega)\Big) \qquad (3\text{-}13)$$

This is the approximate frequency domain expression for the solution of Equation 3-1. It is considered accurate when both α and β are small. The displacement response also can be obtained by inverse Fourier transformation of the Equation 3-13. Equation 3-13 is used in the identification process. Its use will finally lead to the estimation of the parameters from a sequence of measured data.

3.1 Identification Procedure

The method described above provides the solution for the Equation 3-1 in the frequency domain. When the measured values of $f(t)$ are used to estimate $F(\omega)$ and the result is used in Equation 3-13 to obtain $Z(\omega)$, this $Z(\omega)$ will not, in general, match the $Z(\omega)$ estimated from the measured $Z(t)$. Moreover, the calculated $|Z(\omega)|$ will not match the $|Z(\omega)|$ obtained from measurement. The reasons for this mismatch are that (1) noise is inevitably present in the measured input and response. (2) the mathematical model is linear, yet the measured data come from nonlinear structures and (3) the discrete Fourier transform of a time series is used to represent the continuous Fourier transform. In the following, a brief theoretical background is presented together with the simple description of the procedure for finding the unknown parameters.

An equation defining the mismatch between the measured data and the model of Equation 3-1 can be established. Let $|Z^{(m)}(\omega)|$ be the modulus of the Fourier transform of the measured structural response data. Let $|Z(\omega)|$ be the modulus of the function obtained when the Fourier transform of the measured input data is used in Equation 3-13. The difference between these function is defined

$$\epsilon(\omega) = \left|Z(\omega)\right| - \left|Z(\omega)^{(m)}\right| \qquad (3-14)$$

When the discrete Fourier transform is used to approximate the continuous Fourier transform of a measured or theoretical signal, it is defined at a discrete set of frequencies, $\omega_k = k\Delta\omega$, $k = 0,1,\ldots,n-1$. Here n and $\Delta\omega$ relate to the time signal $z(t)$ and its discretization. It is assumed that $z(t)$ is available on the interval $(0, T)$ and is represented by the discrete set of values z_j, $j=0,\ldots/n-1$. Thus, n is the number of points where the signal is represented. $\Delta\omega$ is given by $2\pi/T$. At a particular frequency $\omega = \omega_k$, Equation 3-14 becomes

$$\epsilon_k = \left|Z_k(\omega)\right| - \left|Z_k^{(m)}(\omega)\right| \qquad (3-15)$$

ϵ_k can be positive or negative. A quantity which is always non-negative and which summarizes the differences between the measured, $|Z_k^{(m)}|$, and the theoretical, $|Z_k|$, structural responses in the frequency domain over a range of frequencies is given by

$$\epsilon^2 = \sum_k \epsilon_k^{\,2} \qquad (3-16)$$

This is the square error between measured data and the model. This error can be minimized by properly choosing the parameters, k_0, c_0, α, and β. A method that chooses the parameters this way is a least squares method.

The range of index values, k, over which the above sum is taken, is not specified in Equation 3-16. Equation 3-16 need not be summed from 0 to n. Rather, the summation should be carried out over the range of freuencies which includes those values of Z_k containing significant information on the behavior of the system. In general, this is the band of frequencies surrounding the characteristic frequency of the system.

Now, one can choose k_0, c_0, α, and β, as those constants which satisfy

$$\frac{\partial \epsilon^2}{\partial k_0} = \frac{\partial \epsilon^2}{\partial c_0} = \frac{\partial \epsilon^2}{\partial \alpha} = \frac{\partial \epsilon^2}{\partial \beta} = 0 \qquad (3-17)$$

The k_0, c_0, α, and β, can be located using a search technique. To simplify the analysis, Newton's method is used to minimize ϵ^2 with respect to k_0, c_0, α, and β.

Newton's method converges very rapidly once an iterate is fairly close to the solution. The formal simplicity and its great speed are the reasons why Newton's method is used in this study.

To assure convergence in the numerical analysis, it is important to choose the initial iterate properly. A more detailed discussion of the numerical procedures will be presented later, in the numerical examples.

The steps in the numerical analysis are as follows:

1. Make the initial guesses at the parameter values, k_0, c_0, α, and β.

2. Choose the computation increments Δk_0, Δc_0, $\Delta \alpha$, and $\Delta \beta$.

3. Choose the desired accuracy measure (used to judge convergence).

4. Compute the partial first and second derivatives of ϵ^2 with respect to k_0 using central difference formulas.

5. Use Newton's method to minimize ϵ^2 with respect to k_0.

6. Repeat steps 4 and 5, this time minimizing with respect to c_0, then α, then β.

7. Check the result to convergence.
    a. If convergence has occurred, then stop the analysis.

    b. If convergence has not occurred, then repeat steps 4 through 6.

A computer program to execute the procedure described above has been written. This program is named PUR and a listing is included in the Appendix.

CHAPTER 4

EXAMPLES

4.0 Numerical Examples

In this chapter, numerical examples are presented to demonstrate the use of the previously described analytical procedures. Two examples demonstrating the frequency domain approach to parameter identification are summarized. Both solutions employ the same excitation input. The response signals identified were drawn from two sources. One source was a bilinear hysteretic response while the other was a time varying linear system. Use of these two sources may provide improved understanding of the feasibility of the identification procedure for specific measurements. The examples show the identifications of the parameters for linear and hysteretic, single degree of freedom structures, when measurement noise is and is not present.

The input used to excite the SDF system in all numerical examples is a decaying exponential, oscillatory function. It is generated using the formula

$$f(t) = e^{-\alpha t}\left[\sum_{j=1}^{N} c_j \cos(\omega_j t - \phi_j)\right] \quad 0 \leq t \leq T \qquad (4\text{-}1)$$

Where α, c_j, $j=1,\ldots,N$, and ω_j, $j=1,\ldots,N$ are constants. ϕ_j, $j=1,\ldots N$, are phase angles which are random variable realizations; these random variables are independent and uniformly distributed on the interval $(0, 2\pi)$. α is a decay rate. The c_j, $j=0,\ldots N$, are constants which determine the amplitudes of the excitation. All the values of c_j are taken as equal to c in all cases for the examples. ω_j, $j=1,\ldots N$, are the frequencies where the excitation has power. ω_j, $j=1,\ldots,N$, are equally spaced in the interval including the characteristic frequency of the system being analyzed.

The forcing function defined above was generated at discrete times. Specifically, $f(t)$ was evaluated at the times $t=t_\ell =\ell\Delta t$,

29

l=0,...,N-1. A computer program, named FORCE, which generates
the excitation of Equation 4-1 was used in these numerical
examples.

Two distinct signal types were identified in the numerical
examples. The first example used a computer program, named
BILIN, to compute linear and nonlinear response. BILIN can be
used to find the displacement, velocity, and acceleration
response of a given bilinear hysteretic system to an arbitrary
input. It also computes the energy dissipated by the structure
during the response. The second example used a computer program,
named TIMEVA, to compute the response. This program computes a
linear time dependent response defined by Equations 3-1 and 3-2
with α, β, c_0, and k_0, constants.

White noise was used whenever measurement noise was added to
the signals. The white noise is normally distributed, $N(0,\sigma_n^2)$
A subroutine named NOISE was used to generate the noise signal.
The noise signals were added to the generated input and response
signals in the following manner. First, the excitation and
response signals were generated using programs FORCE and BILIN or
TIMVA. Then noise/signal ratios were selected and used to obtain
the variances of the noise signals. The noise signals were
generated as sequences of independent random variables, and
directly added to the excitation and response. These noisy
signals were then used as inputs to do the identification. Note,
no filtering procedure was used on the simulated measured signals
during the identification process.

Three basic models to represent the hysteretic system were
pursued in this study. All the model parameters were identified
in the frequency domain. The identification procedures and
formulations were described previously. Different identification
approaches may be applied for the same model. Three computer

30

programs, FREQID, PUR3 and PUR, were written to execute the parameter identifications.

FREQID performs approximate frequency domain parameter identification for second and third order linear models. It accepts both an input signal from FORCE and a response signal from BILIN or TIMEVA. When desired, the white noise signals are added to the corresponding input data. Then FREQID performs the necessary Fourier transforms and other data operations. Following this, the parameter identification is executed. One operation required in the parameter identification is estimation of the characteristic frequency. This can be done simply by searching $Q(\omega) + \epsilon(\omega)$ for a minimum value. However, a more precise method for determining the minimum value of $Q(\omega) + \epsilon(\omega)$ defined in Equation 2-13 and 2-16 involves use of a least square method. In this improved method, $Q(\omega) + \epsilon(\omega)$ terms are fit into a polynomial model where frequency is the only variable. Once the coefficients for this equation are estimated, the equation representing the $Q(\omega) + \epsilon(\omega)$ is used to identify the characteristic frequency and other parameters.

An important assumption was made for the third-order model, Equation 2-26. In particular, it was assumed that a_2 is small in value. This assumption was used in FREQID. The parameters of this model may be identified, without the assumption that a_2 is small, by the search technique. The computer program PUR3 was written for this purpose. A detailed description of this method was given in Chapter 3.

Program PUR performs parameter identification for second-order time varying linear systems. The approach is based on the procedure described in Chapter 3. The program accepts the inputs and responses generated in the programs FORCE and BILIN or TIMEVA, with or without noise. Four parameters, namely k_0, α,

31

c_0, and β are identified. The program employs a search technique; the initial estimators can be chosen by using the identified parameters obtained from any of the methods.

Once the parameters have been estimated, the energy dissipated by the model is computed. This result together with the predicted response is compared to both the energy dissipated and the response of the actual system. The energy and response computations are performed in program ENER2 and ENER3 for the second and third order system, respectively.

From the above description, the methods used in the determination of the system parameters can be summarized as follows:

Method 1. Performs parameter identification for the second-order system in the frequency domain utilizing Equation 2-20. No fitting equation for $Q(\omega) + \epsilon(\omega)$ is applied.

Method 2. Performs parameter identification for the third-order system in the frequency domain utilizing the equations from 2-32a to 2-35. No fitting equation for $Q(\omega) + \epsilon(\omega)$ is applied.

Method 3. Performs parameter identification using the same approach as Method 1 except the input data $Q(\omega) + \epsilon\omega$ are replaced by the fitted polynomial equation. This additional analysis is done in a subroutine called FIT.

Method 4. Performs parameter identification using the same approach as Method 2 and using the same procedure described in Method 3.

Method 5. Performs parameter identification for the third-order system using the search method described in Chapter 3. The operation is executed in a program called PUR3. Prior estimates obtained from the above methods are used.

32

Method 6. Performs parameter identification for the second-order time-varying parameter system in the frequency domain. The search method described in Chapter 3 is used. This method also requires prior estimators which can be obtained from the information supplied in Methods 1 through 5.

All the methods described above can be used to estimate the parameters for the linear and nonlinear systems even when noise is present. The duration of the excitation must be long enough to characterize the system parameters.

In the following numerical examples, four basic problems are solved. These cases involving different degrees of nonlinearity in the system response are summarized below.

Case 1. An input excitation is generated using Equation 4-1. The input is used to excite a linear SDF system with viscous damping. The excitation and linear response are used to identify the model parameters. Noise signals can be added to the generated input and response, if required.

Case 2. An excitation input is generated as in Case 1, but here the repsonse of a bilinear hysteretic system is computed. Yielding occurs in the response. The degree of nonlinearity was designed using a comparison between the yield displacement of the bilinear system and the maximum displacement of the linear system. Let the yield displacement of the bilinear system be z_y. Let the maximum displacement of the linear system be z_{max}. In this case, z_{max} is taken as 6.7 and z_y is equal to 6.0.

Case 3. Same as Case 2, but z_y is equal to 5.0.

Case 4. Same as Case 2, but z_y is equal to 4.0.

Case 5. An input excitation is generated as in Case 1. The input is used to excite a linear SDF system with time varying damping and stiffness. The excitation and response are used to identify the model parameters. Noise signals are added to the simulated input and response when required.

4.1 Example 1

This example carries out the parameter identification using the methods described above. Specifically, methods 1 through 6 are used to identify the parameters. The parameters of the input excitation are listed in Table 4.1. The notation for the parameters was specified above.

TABLE 4.1. PARAMETERS OF THE FORCING FUNCTION

$\alpha = 0.1$ $N = 50$ $c_j = 10.0$ $j = 1,..,50$

$\omega_j = (1.8 + 0.008j)\pi$ $,j = 1,...50$

$\Delta t = 0.05$ $n = 1024$

A typical forcing function history generated by using these parameters is shown in Figure 4.1. Actual forcing functions measured in the field usually contain a certain amount of noise. Inputs with noise to signal ratios of six and eight percent are shown in Figures 4.2 and 4.3, respectively.

The response of some SDF systems to the forcing input were computed. The energy dissipated in each structure is listed with the structural parameters in Tables 4.1A and 4.1B. All cases were described above. The notation of the system parameters is as follows: k is the initial stiffness; c is viscous damping; k_y is the yield stiffness; z_y is the yield displacement; z_{max} is the maximum displacement of an SDF system; m is the mass of the SDF structure.
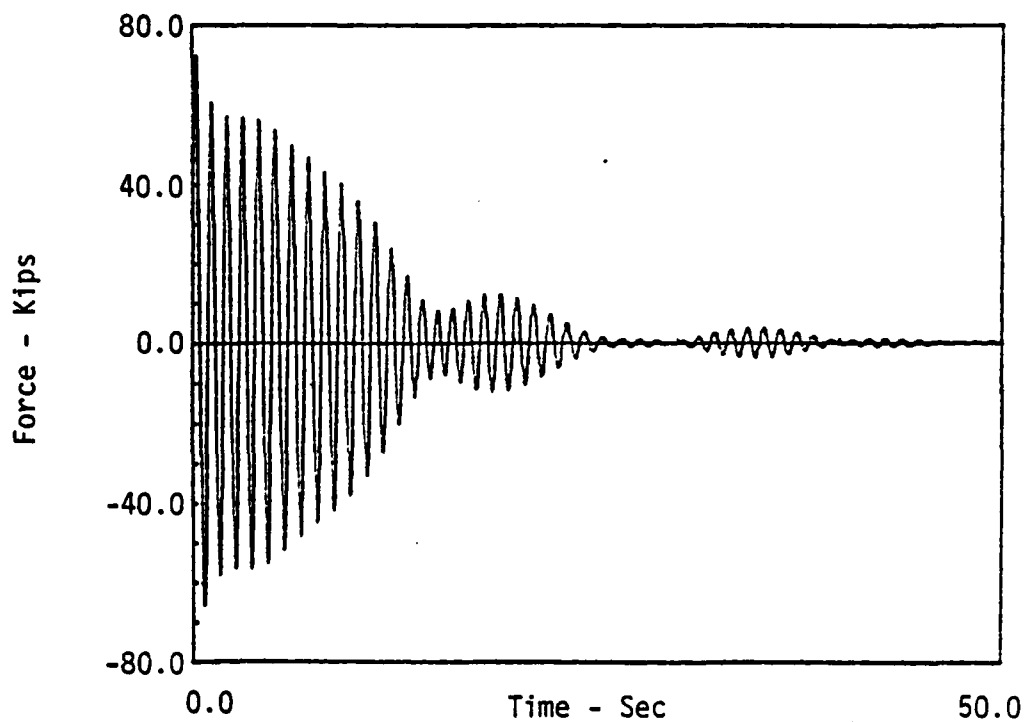
Figure 4.1   Signal used to simulate the actual
input in Examples 1 and 2
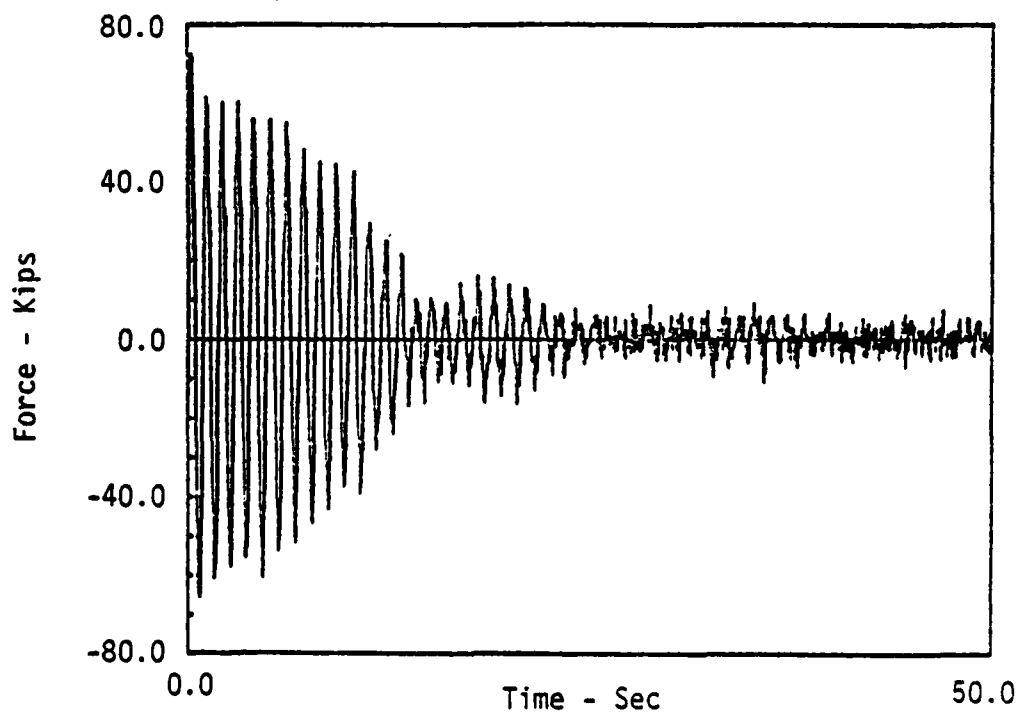
Figure 4.2   Signal used to simulate the measured
input.   (Includes 6% noise)

35
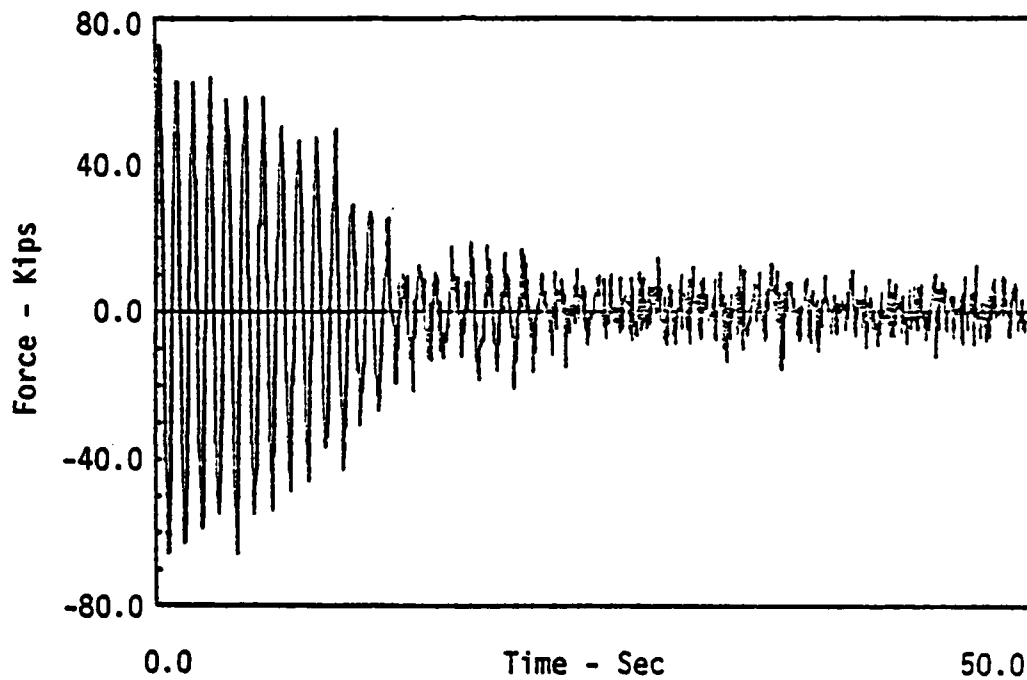
Figure 4.3 Signal used to simulate the measured
input. (Includes 10% noise)

TABLE 4.1A. SYSTEM PARAMETERS

$$k = 39.48 \qquad c = 1.257 \qquad m = 1.0$$
$$z_{max} = 6.7 \qquad k_y = 0.0 \qquad \Delta t = 0.05 \qquad n = 1024$$

TABLE 4.1B. ENERGY DISSIPATION FOR CASE 1 THROUGH CASE 4

Cases	z_y	Damping Energy Dissipated	Spring Energy Dissipated	Total Energy Dissipated
Case 1	∞	11028.20	0.0	11028.2
Case 2	6	10199.30	405.21	10604.0
Case 3	5	8364.27	1186.74	3551.0
Case 4	4	6300.53	1924.48	8225.0

First, the response of a linear system (case 1) was computed. Then, a slightly nonlinear response of an SDF structure was computed for analysis in case 2. The displacement response versus time for case 2 is plotted in Figure 4.4. The spring restoring force versus displacement is shown in Figure 4.5. A small plastic deformation is shown. The total restoring force versus displacement is plotted in Figure 4.6. The measured responses for Case 2 with a certain amount of noise are plotted in Figures 4.7 and 4.8. Figure 4.7 shows a measured signal with six percent noise to signal ratio. Figure 4.8 shows a measured signal with ten percent noise to signal ratio. Two more severe nonlinear responses were computed for analysis in cases 3 and 4.

The displacement response versus time for case 4 is plotted in Figure 4.9, and the measured response for case 4 with ten percent noise to signal ratio is shown in Figure 4.10. The spring restoring force versus displacement is shown in Figure 4.11. A considerable permanent set is evident in Figure 4.9. Figure 4.11 shows that plastic deformation occurs in the structure in both directions of motion.
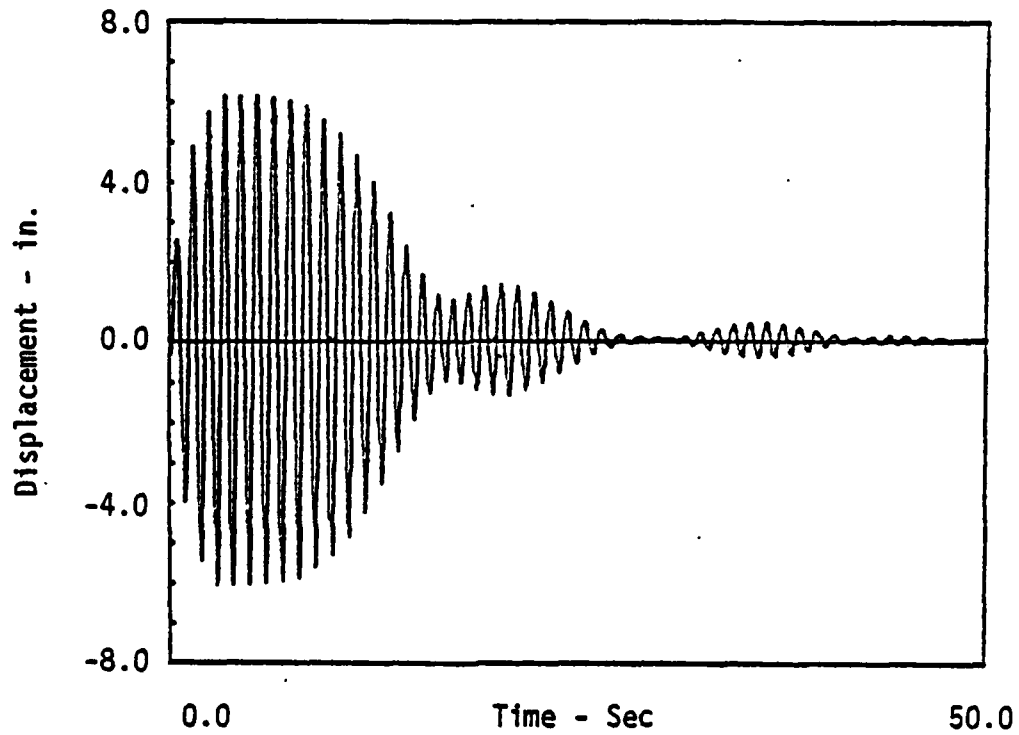
Figure 4.4 Displacement response of nonlinear
SDF system to force in Figure 4.1
(Case 2)
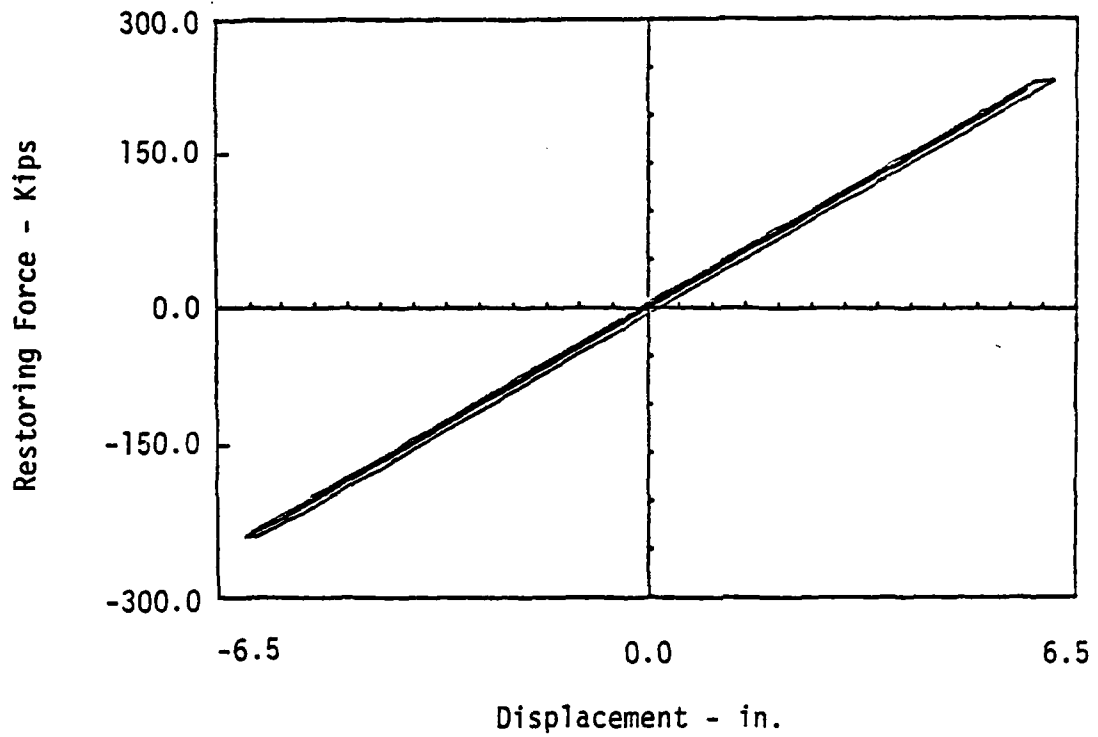
Figure 4.5   Spring Restoring Force versus displacement for nonlinear system (Case 2)
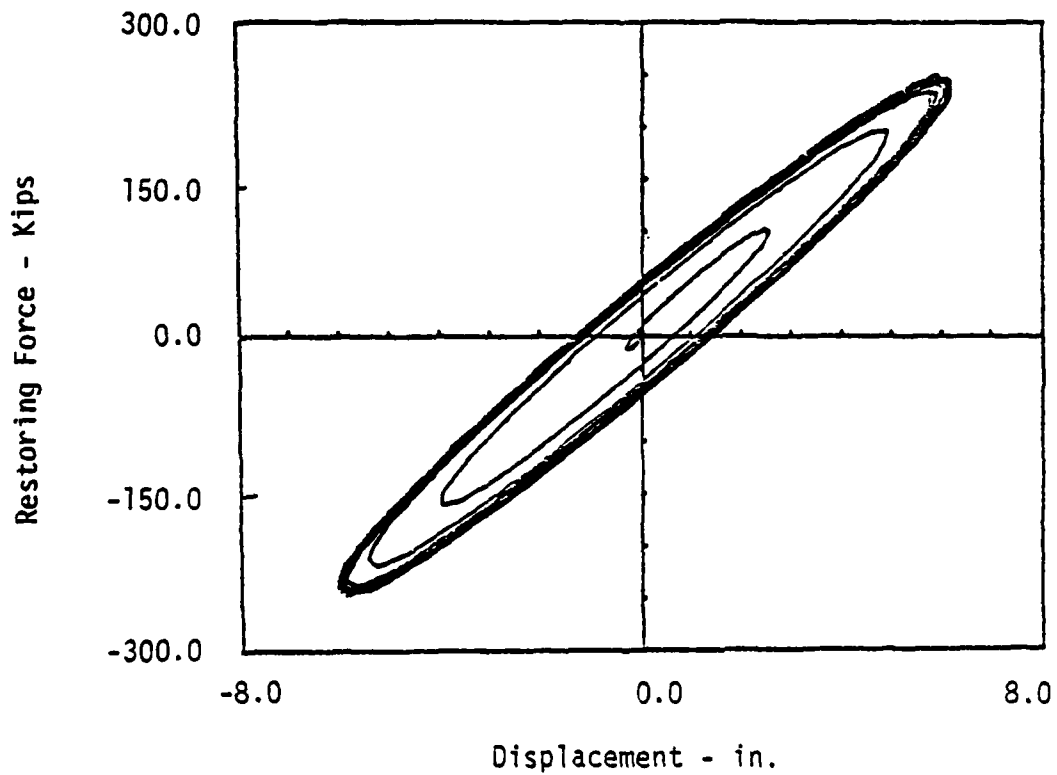
Figure 4.6   Spring plus damper restoring force versus displacement (Case 2)
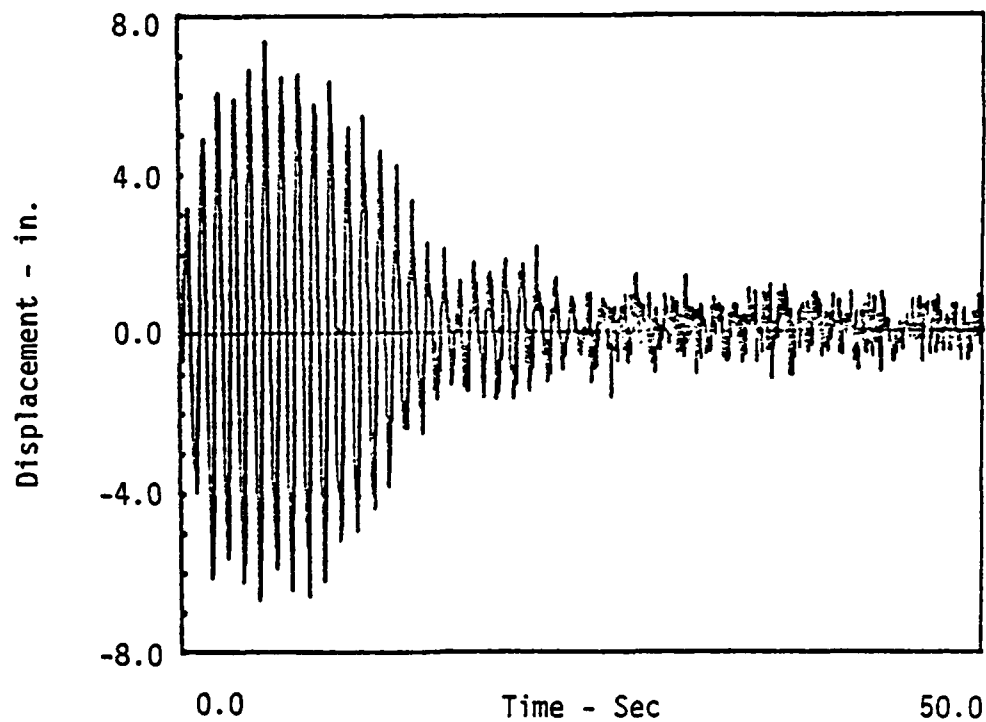
Figure 4.7   Signal used to simulate measured
displacement response.   Signal of
Figure 4.4 plus 6% noise
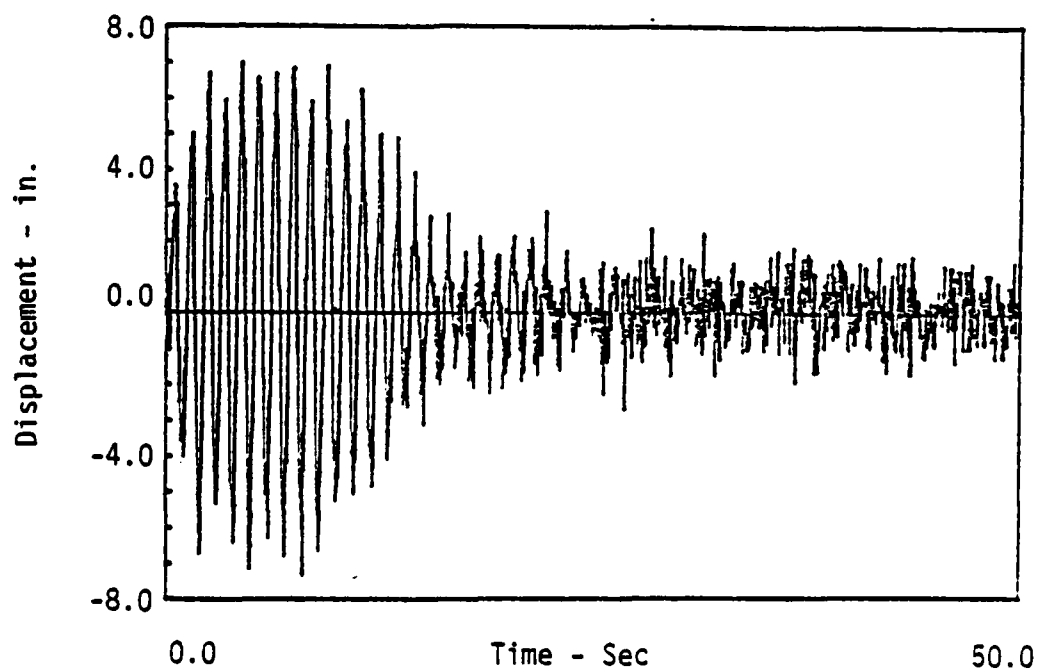
Figure 4.8   Signal used to simulate measured
displacement response.   (10% noise)

40
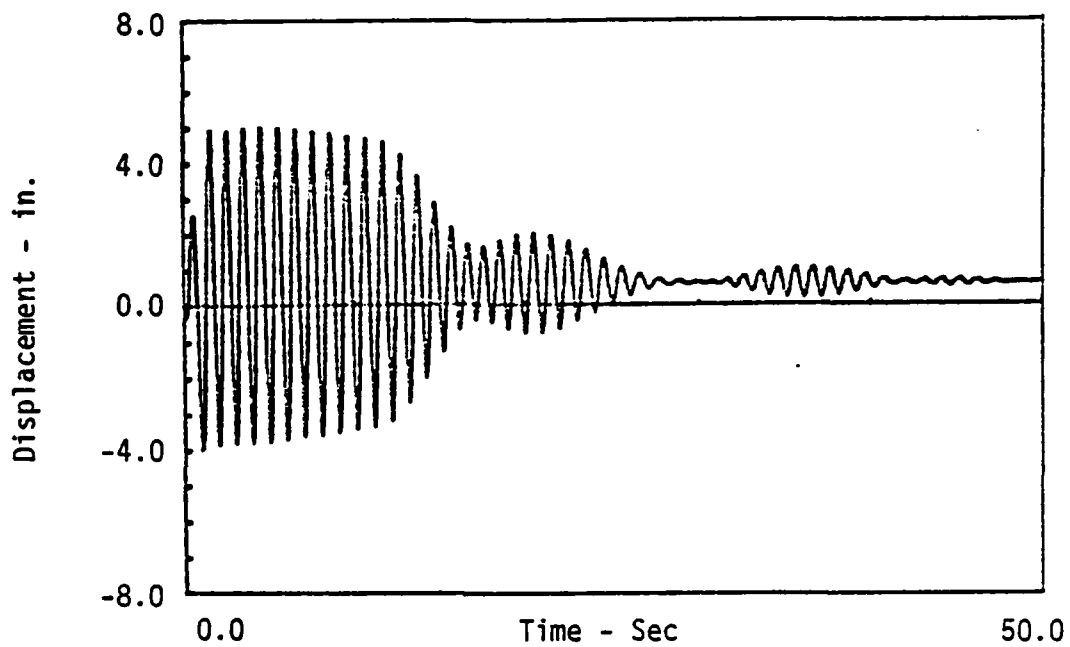
Figure 4.9   Displacement response of nonlinear system
              to the force in Figure 4.1 for Case 4
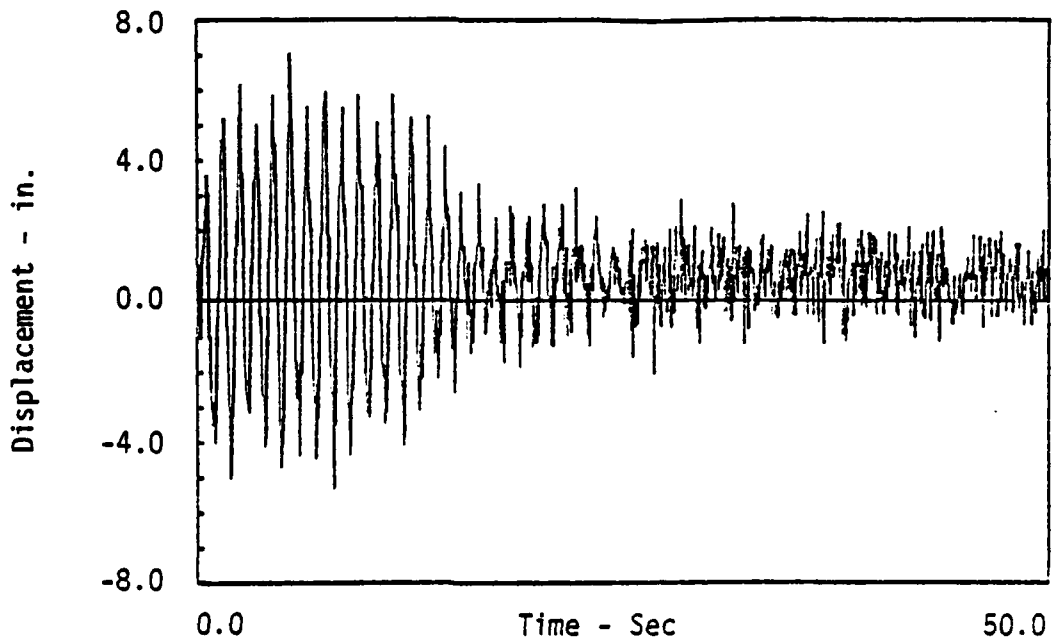
Figure 4.10   Displacement response (Case 4) plus
              10% noise

41
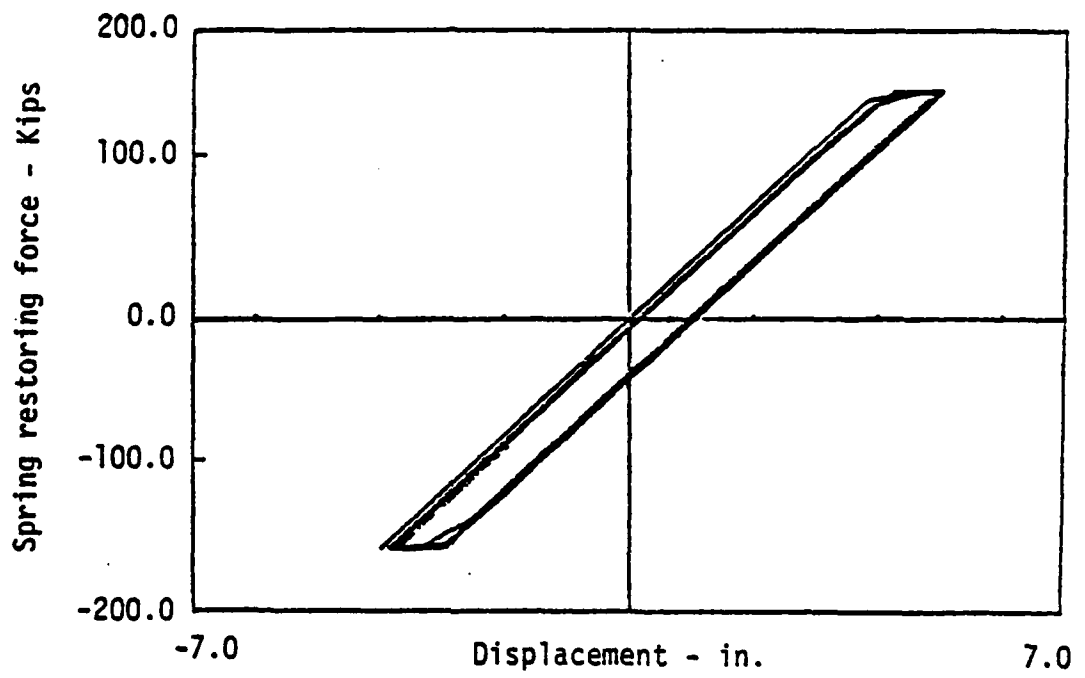
Figure 4.11   Spring restoring force versus displacement for nonlinear system (Case 4)

Using the forcing function input, described above, and the computed responses, the parameters of the structures were identified. The results of the parameter identification are given in Tables 4.2 through 4.5. These results provide the identified parameters in the noise-free case. The energy dissipated by the identified system is listed next to the identified parameters. For method 6, the parameters a_0, a_1, a_2, and α_3 identify with the parameters k_0, β, c_0, and α, respectively.

TABLE 4.2. IDENTIFIED PARAMETERS AND ENERGY
DISSIPATED FOR CASE 1.

Method	a_0	a_1	a_2	a_3	Energy
1	39.17	1.26			11210.0
2	39.17	1.28	0.0		11090.0
3	40.01	1.28			10720.0
4	40.01	2.48	0.0236		9270.0
5	39.50	1.26	0.0		11200.0
6	39.33	0.0	1.274	0.0	10741.0

TABLE 4.3. IDENTIFIED PARAMETERS AND ENERGY
DISSIPATED FOR CASE 2

Method	a_0	a_1	a_2	a_3	Energy
1	33.27	1.45			7968.0
2	33.27	3.98	0.05		7028.0
3	35.84	1.28			10500.0
4	35.84	3.57	0.042		7690.0
5	34.27	3.68	0.062		10370.0
6	36.56	0.001	1.094	0.022	10077.0

TABLE 4.4. IDENTIFIED PARAMETERS AND ENERGY DISSIPATED FOR CASE 3

Method	a_0	a_1	a_2	a_3	Energy
1	33.27	1.35			7802.0
2	33.27	2.98	0.032		7368.0
3	35.32	1.41			9482.0
4	35.32	2.74	0.027		8185.0
5	32.54	2.98	0.042		8324.0
6	40.21	- 0.0013	1.589	- 0.018	9661.0

TABLE 4.5. IDENTIFIED PARAMETERS AND ENERGY DISSIPATED FOR CASE 4

Method	a_0	a_1	a_2	a_3	Energy
1	33.27	1.67			7376.0
2	33.27	2.28	0.014		7053.0
3	34.61	1.75			7703.0
4	34.61	2.50	0.018		7486.0
5	30.30	3.95	0.066		7598.0
6	40.26	- 0.0018	1.708	0.001	8186.5

Section 4.0 demonstrated that when the higher order linear model is used to simulate the actual system behavior, the parameter a_0 must be estimated first in the identification procedures, methods 1 through 4. The estimation of this parameter can be executed either by simply searching for a minimum in $Q(\omega) + \epsilon(\omega)$, or by using a curve-fit to $Q(\omega) + \epsilon(\omega)$, and then finding the minimum of the curve. Figure 4.12 shows a realization of $Q(\omega)$ for a specific case. This is the ratio of the Fourier transform moduli of the structure input and response. An example of the quantity $Q(\omega) + \epsilon(\omega)$ is shown in Figure 4.13. It

400.0

$Q(\omega)$

200.0

0.0

4.0   6.0   8.0

Frequency(ω) – Second/cycle
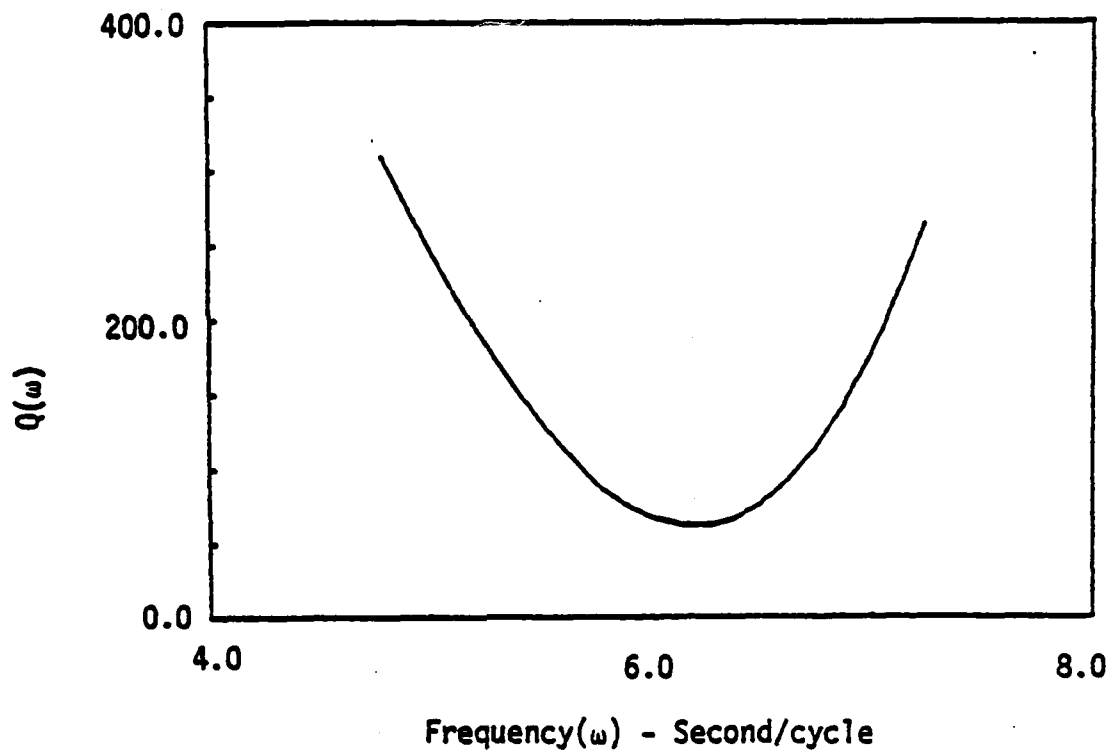
Figure 4.12   A realization of $Q(\omega)$

600.0

$Q(\omega) + \epsilon(\omega)$

300.0

0.0

4.0   6.0   8.0

Frequency(ω) – Second/cycle
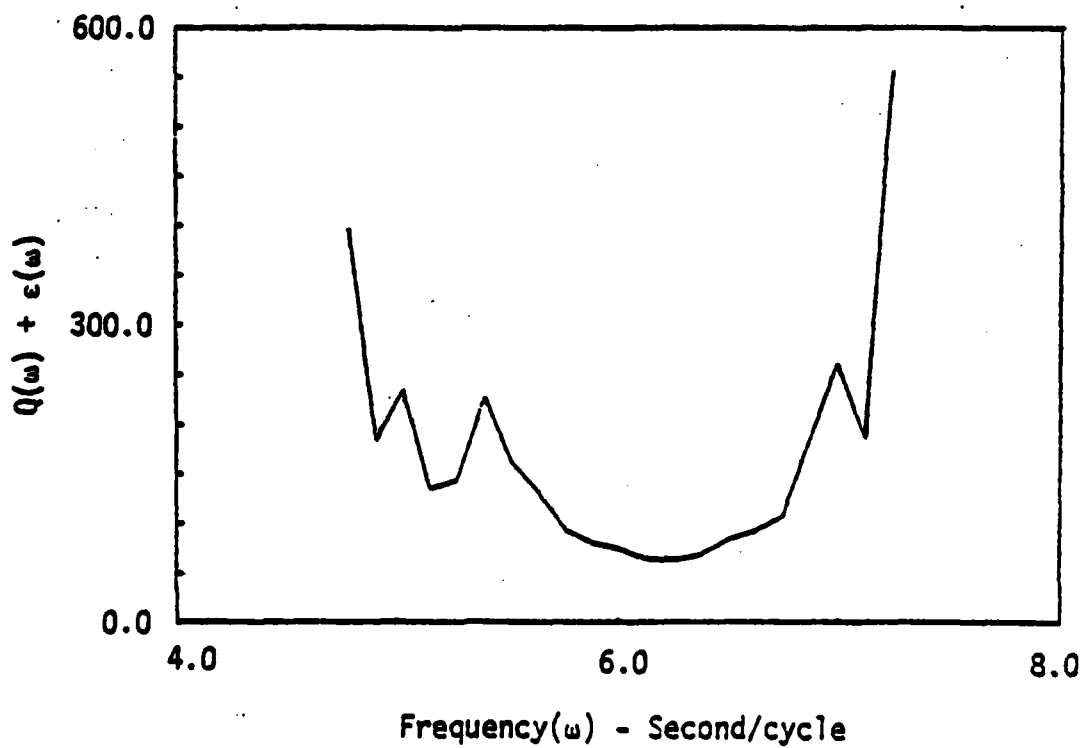
Figure 4.13   A realization of $Q(\omega) + \epsilon(\omega)$

45

is apparent from this diagram why the use of a curve-fit provides better results.

Figures 4.14 through 4.16 show comparisons between the responses of the identified systems computed by different methods, and the actual response of the bilinear hysteretic system in case 2. The responses of the identified systems match the response of the actual system so closely that it is difficult to distinguish the two responses in these figures. More identified responses for case 4 are shown in Figures 4.17 through 4.19. The model responses do not match the actual response as closely when residual deformation exists in the actual structure since the models cannot accumulate permanent deformation. However, peak responses in the models match the actual system response quite well.

In this example, noise was added to the forcing function and response signals; then the system parameters were identified. The results are summarized in Tables 4.6 and 4.7.

TABLE 4.6. IDENTIFIED PARAMETERS AND ENERGY DISSIPATED
FOR CASE 1 WITH TEN PERCENT NOISE TO SIGNAL RATIO

Method	a_0	a_1	a_2	a_3	Energy
1	39.17	1.37			11022.0
2	39.17	1.45	0.003		10900.0
3	39.93	1.42			10300.0
4	39.93	2.44	0.022		9497.0
5	34.30	2.98	0.051		11710.0
6	38.44	0.0	1.286	0.0	10929.0
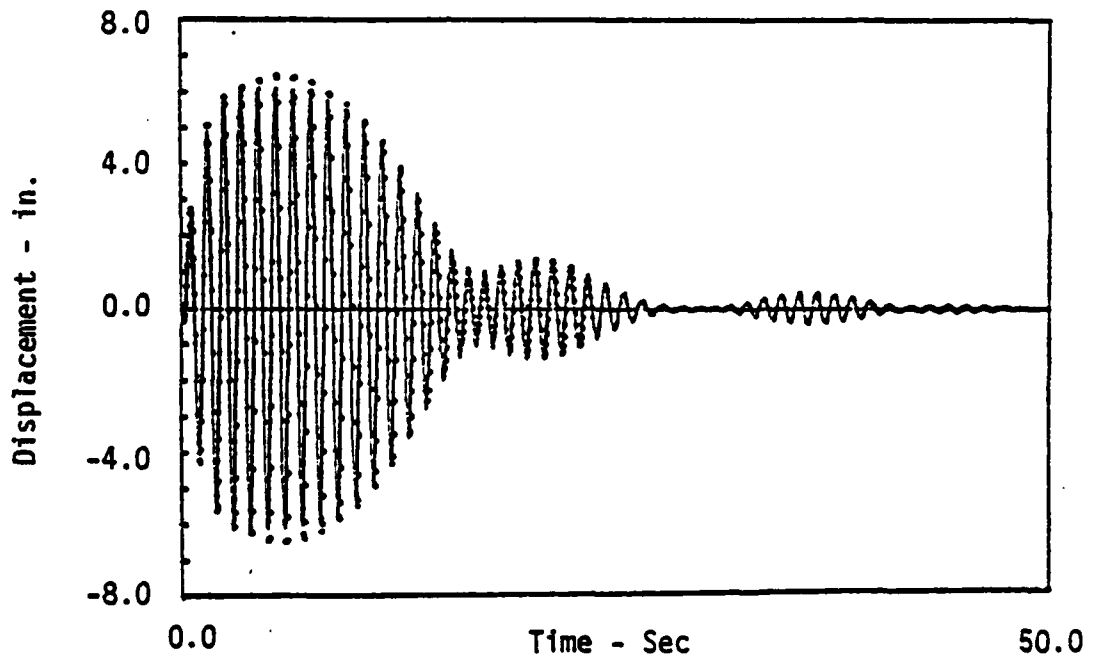
Figure 4.14   The comparison between noise-free
response (solid) and Second-order
identified response (dot) for Case 2

47
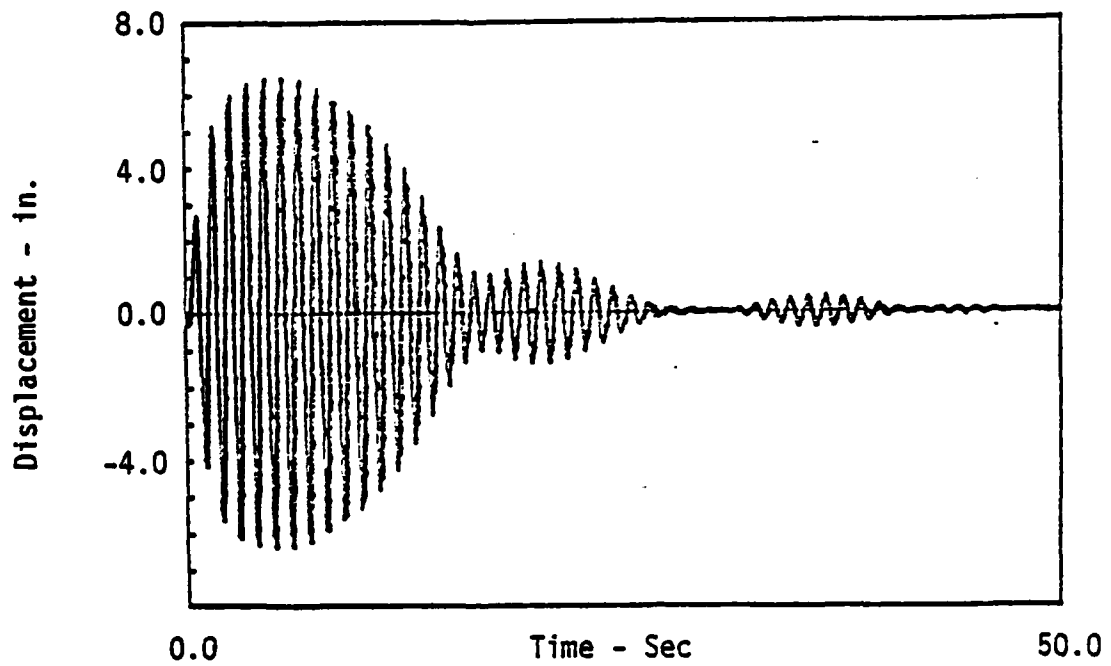
Figure 4.15   The comparison between noise-free response (heavy) and third-order identified response (light) for Case 2
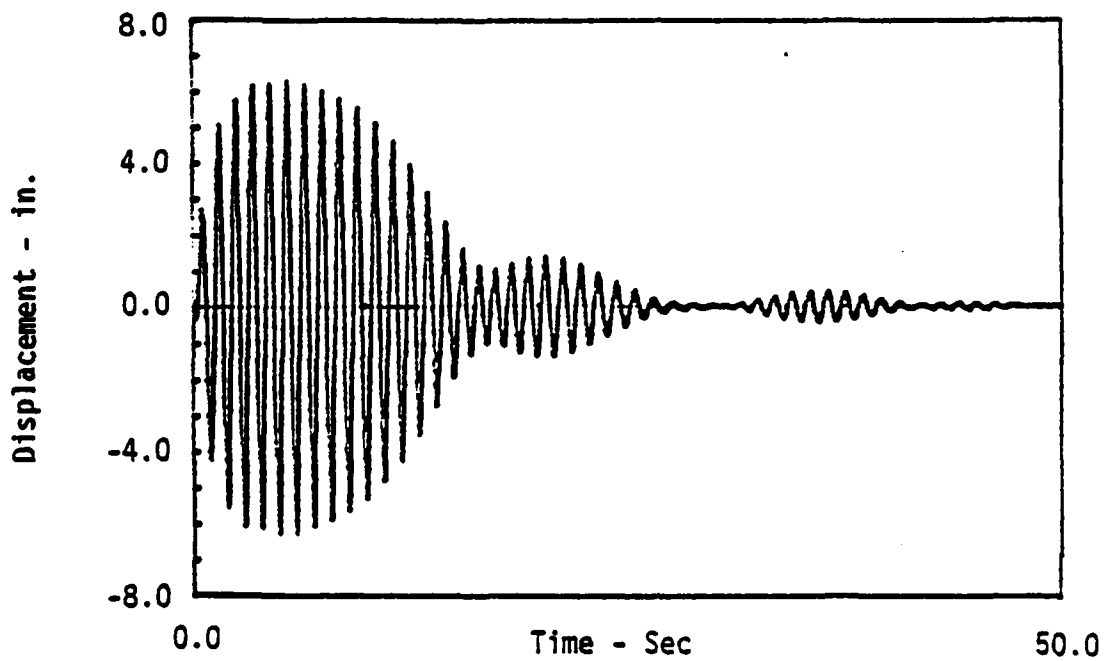
Figure 4.16   The comparison between noise-free response (heavy) and second-order time varying parameters identified response for Case 2

48
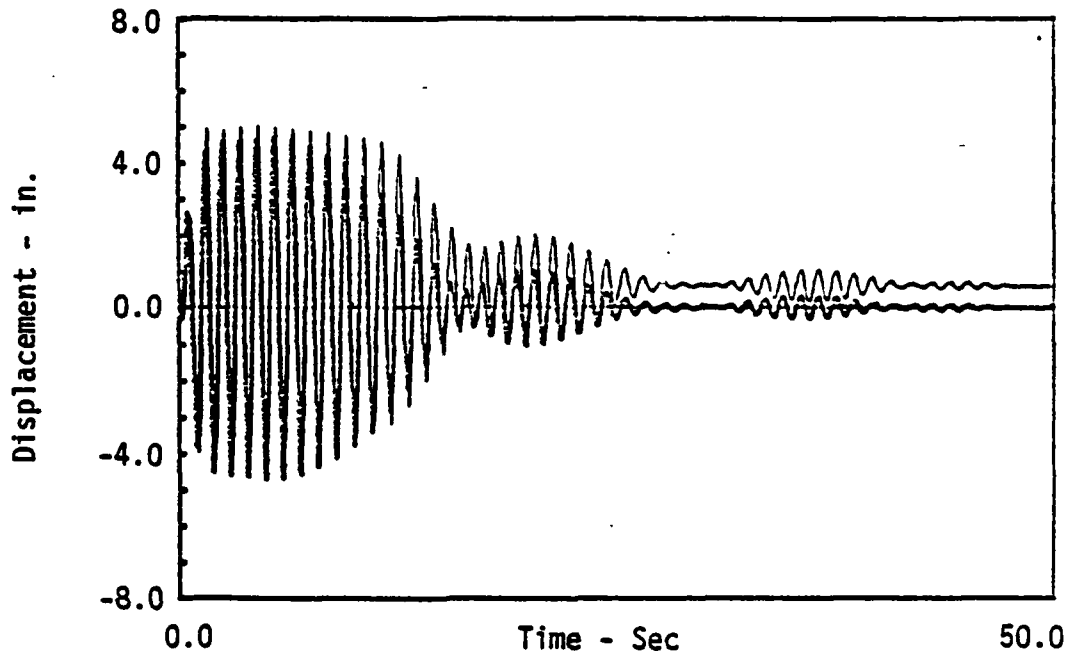
Figure 4.17   Comparison between actual response (thin line) and model (method 3) response (thick line)
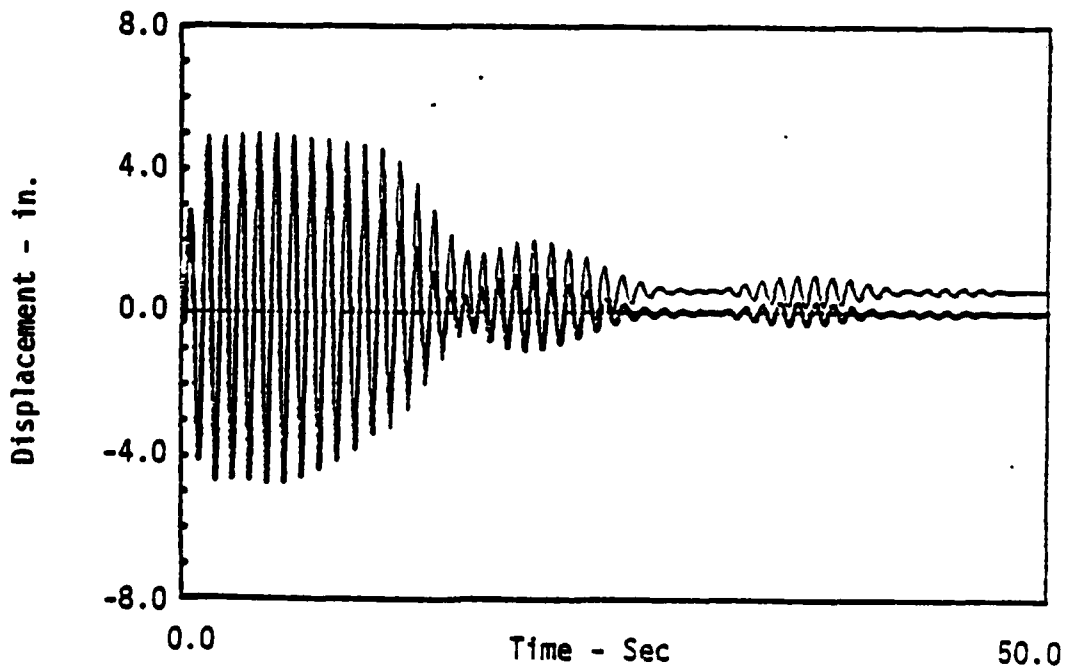
Figure 4.18   Comparison between actual response (thin line) and model (nethod 5) response (thick line)

49
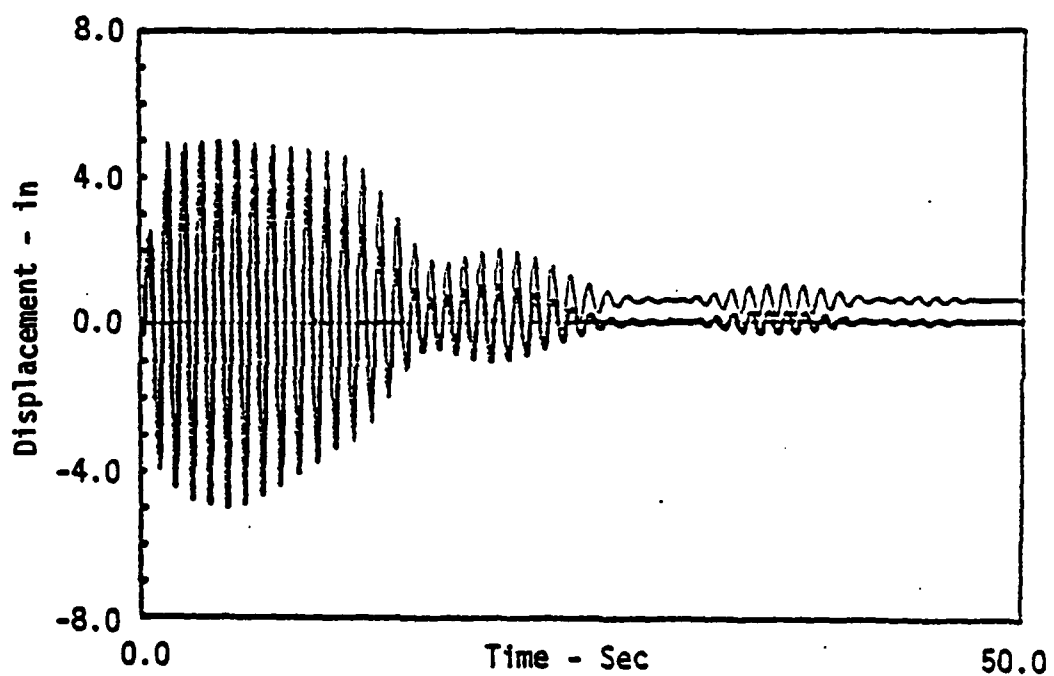
Figure 4.19 Comparison between actual response
(thin line) and model (method 6)
response (thick line)

TABLE 4.7. IDENTIFIED PARAMETERS AND ENERGY DISSIPATED
FOR CASE 4 WITH TEN PERCENT NOISE TO SIGNAL RATIO

Method	a_0	a_1	a_2	a_3	Energy
1	33.27	1.89			7092.0
2	33.27	1.42	0.021		9980.0
3	32.02	1.95			6476.0
4	32.02	2.60	0.021		6803.0
5	34.46	2.70	0.043		11400.0
6	32.83	0.0026	1.543	0.011	7016.0

These results show that the parameter identification procedure is
still effective when noise is present.

4.2 Example 2

In this example, a parameter identification problem is
solved using the frequency domain approach. The methods used to
identify the parameters were described in section 4.0, namely
methods 1 through 6. The same forcing function as illustrated in
Example 1 is used. The only difference in this example is that
the response was simulated by a second-order time varying param-
eter system. Unlike the responses simulated in Example 1, this
example is a linear system with time dependent stiffness and
damping. The parameters of the system and total energy dissi-
pated are listed in Table 4.8.

TABLE 4.8. SYSTEM PARAMETERS FOR CASE 5

$k_0 = 39.48$ $c_0 = 1.257$

$\beta = -0.01$ $\alpha = 0.01$

Total Energy = 9799.0

The definitions of the symbols are the same as in Equation 3.2.
This case was described in section 4.0 as case 5.

The displacement response versus time for case 5 is shown in Figure 4.20. The total restoring force versus displacement for this case is illustrated in Figure 4.21. Note that the major axis of the loops depicted in the diagram have different slopes. This occurs because the system stiffness diminishes with time. The parameters identified using methods 1 through 6 together with the total energy dissipated in the corresponding systems are shown in Table 4.9.

TABLE 4.9. IDENTIFIED PARAMETERS AND ENERGY
DISSIPATED FOR CASE 5

Method	a_0	a_1	a_2	a_3	Energy
1	34.70	1.36			9266.0
2	34.70	3.25	0.039		7883.0
3	37.15	1.29			10960.0
4	37.15	2.82	0.031		9074.0
5	34.31	2.97	0.05		11160.0
6	37.56	- 0.006	1.23	0.019	9120.2

It is shown that methods 1 through 6 can also be used to identify model parameters when noise is present. The results obtained when the measured signals contain noise are shown in Table 4.10.

TABLE 4.10. IDENTIFIED PARAMETERS AND ENERGY DISSIPATED
FOR CASE 5 WITH SIX PERCENT NOISE TO SIGNAL RATIO

Method	a_0	a_1	a_2	a_3	Energy
1	34.70	1.38			9419.0
2	34.70	2.75	0.03		8623.0
3	37.34	1.31			11180.0
4	37.34	2.24	0.021		10280.0
5	34.32	2.49	0.038		11040.0
6	38.30	- 0.007	1.254	0.025	9245.6
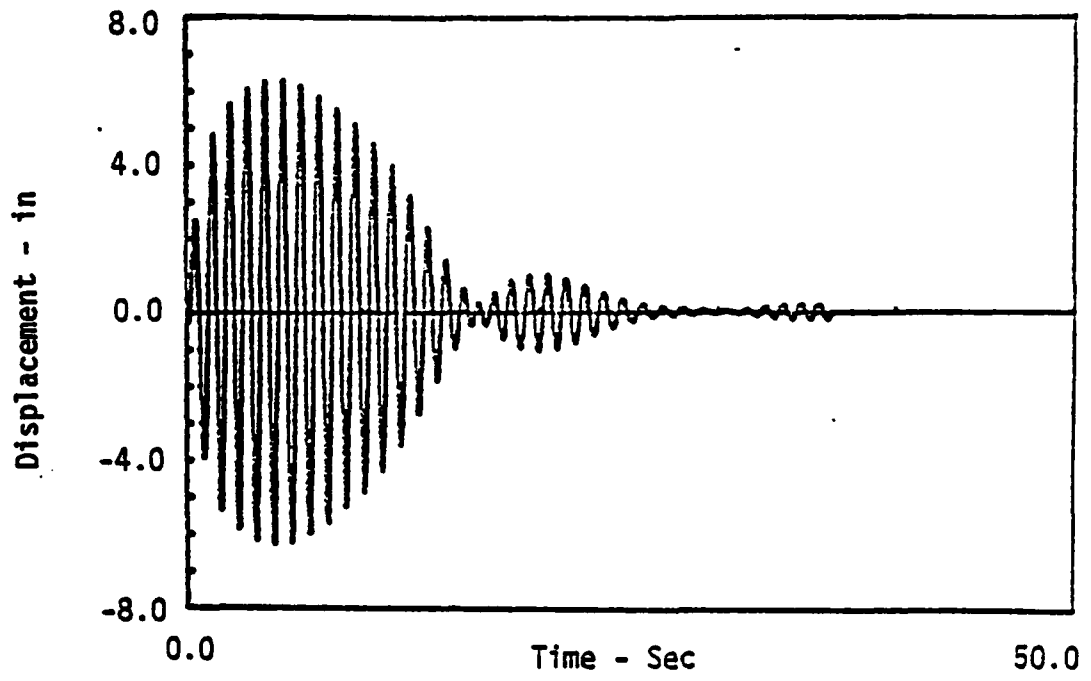
Figure 4.20   Displacement response of second-order
time varying parameter system to force
in Figure 4.1 (Case 5)
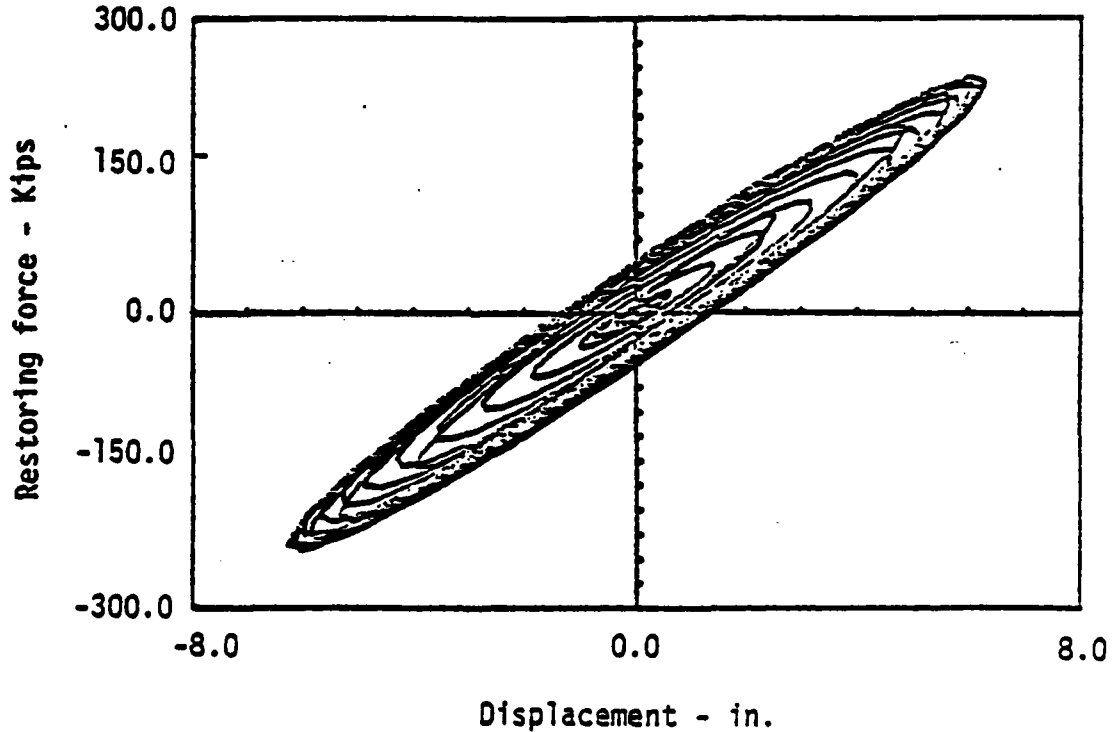
Figure 4.21   Total restoring force versus displace-
ment for time varying parameter system
(Case 5)

Figures 4.22, 4.24, and 4.25 compare the identified system responses to the response of the actual system. The simulated and actual responses match quite well in all cases. The model including time parameters provides the best match. Figure 4.23 shows the total restoring force versus displacement. A change in slope of the major axis of the loops is observed. This behavior matches the real system behavior shown in Figure 4.21.
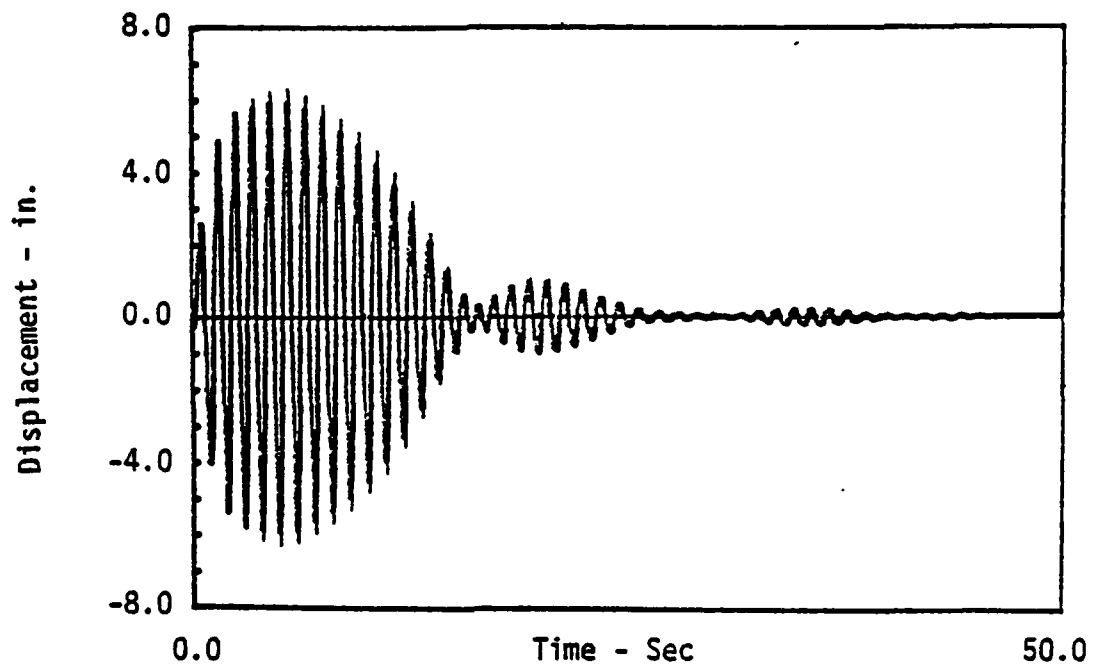
Figure 4.22   The comparison between measured response
               (light) and the identified response
               (dark) by method 6 for Case 5
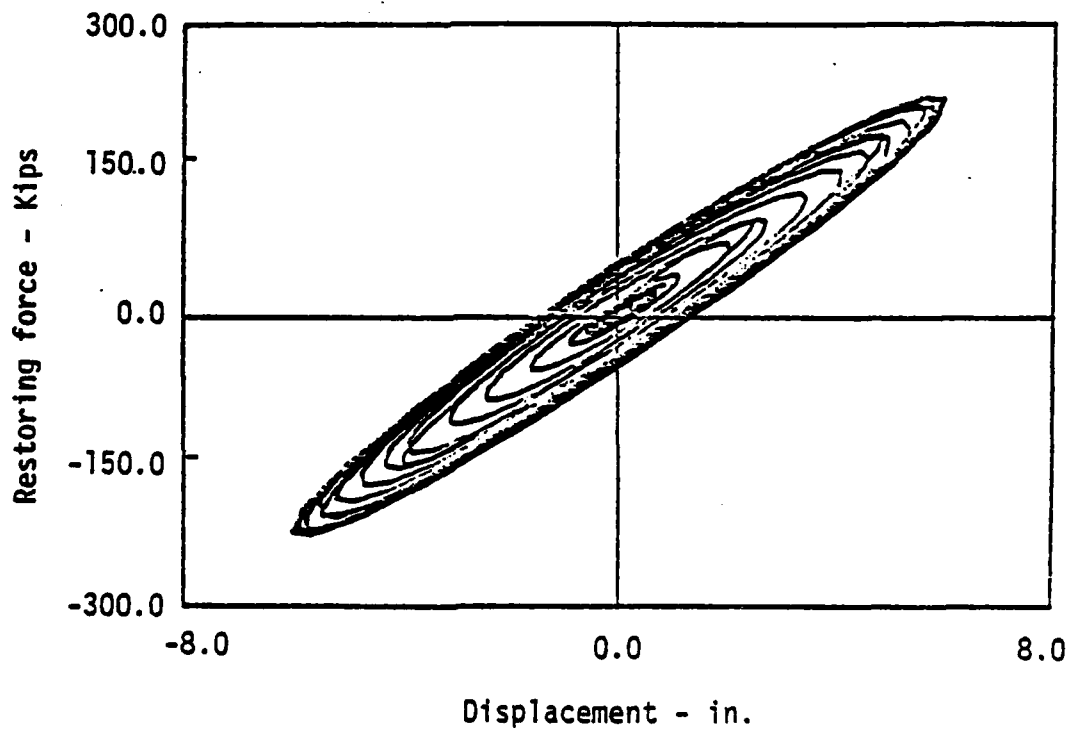
Figure 4.23   Total restoring force versus displace-
               ment after the identification by using
               method 6 for Case 5

55
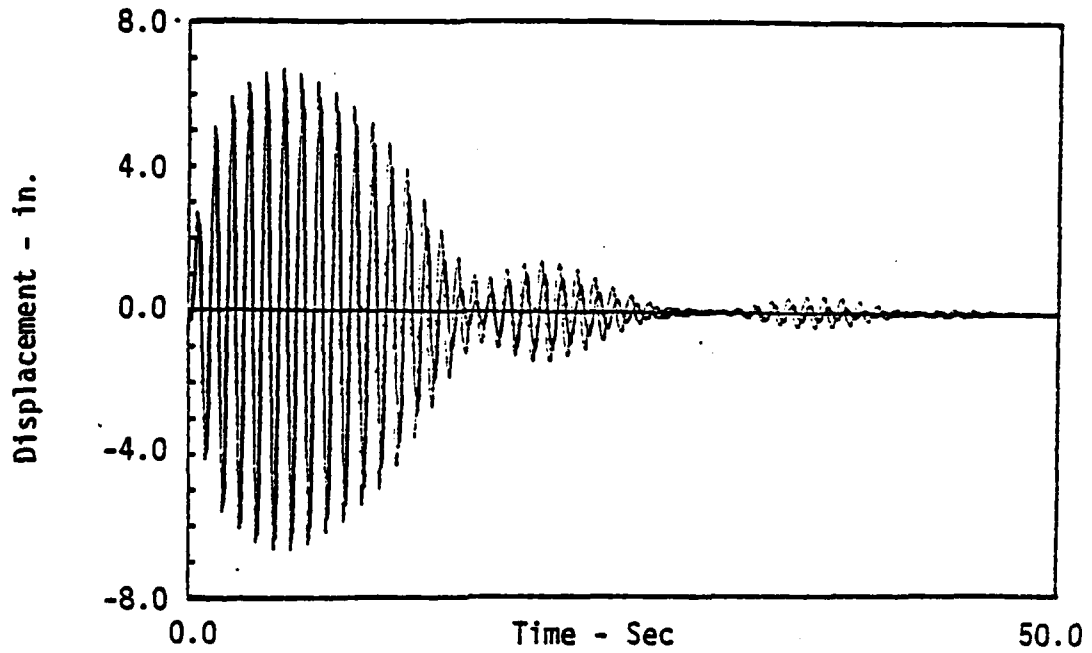
Figure 4.24   Comparison between measured response
(heavy) and second-order identified
response (light) using method 3 for
Case 5
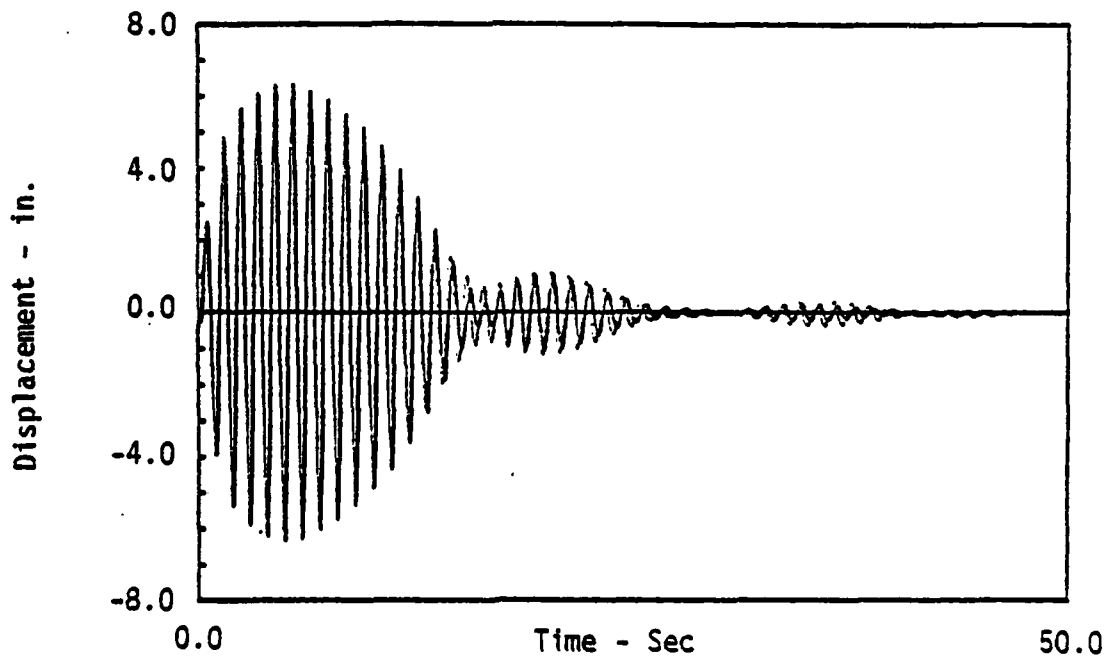
Figure 4.25   Comparison between measured response
(heavy) and the third-order response
(light) using method 4 for Case 5

CHAPTER 5
SUMMARY AND CONCLUSIONS

The objective of this study was to develop approximate linear models for the simulation of inelastic system response and the measurement of damage accumulation in a structure. It was assumed that energy dissipated is related to the accumulation of damage. The model parameters were identified; then the energy dissipated during a strong motion was calculated. The displacement response and the energy dissipated in each model were compared with the displacement response and energy dissipated in the actual structure.

Three basic models were considered in this study. These are second and third order linear models with constant coefficients, and a second order linear model with time-varying parameters. The frequency domain approach was used in all the parameter identification computations.

Several numerical examples were solved. The results obtained lead to the following conclusions:

1. Linear and nonlinear hysteretic SDF systems can, in some respects, be accurately modeled using second- and third-order linear differential equations with constant coefficients, and a second-order linear differential equation with time-varying coefficients. Specifically, the models provide accurate simulations when displacement response and energy dissipated criteria are used.

2. The frequency domain approach can be used to identify model parameters of all three models when the force and response measuements are noisy.

3. The second order model with time-varying coefficients provides the best simulation of system response and energy dissipated among the three models considered.

While the procedures developed in this investigation provide means for the simulation of response and the estimation of damage in inelastic structures, some improvements can be made. The systems considered in this study are SDF; future investigations should include multi-degree-of-freedom structures. The models used in this study do not permit the accumulation of plastic deformation; future investigations should consider models that allow plastic deformation to accumulate. The tests that are summarized in the appendix show that material damage is related to energy dissipated; further experiments should be performed, and a mathematical model characterizing the results should be developed. Finally, analyses should be performed to establish the special distribution of energy dissipated in actual structural members.

REFERENCES

1. Lutes, L. D., "Equivalent Linearization for Random
   Vibration," Journal of the Engineering Mechanics Division,
   ASCE, Vol. 96, No. 6M3, June 1970, pp. 227-242.

2. Lutes, L. D. and Hseih, J., "High Order Equivalent
   Linearization in Random Vibration," Proceedings, Third
   Engineering Mechanics Division, Special Conference, Austin,
   Texas, September 17-19, 1979, pp. 60-63.

3. Wen, V. K., "Stochastic Response Analysis of Hysteretic
   Structures," Proceedings of the Specialty Conference on
   Probabilistic Mechanics in Structural Reliability, ASCE,
   Tucson, Arizona, January 1979.

4. Wen, V. K., "Method for Random Vibration of Hysteretic
   Systems," Journal of Engineering Mechanics, Div. Proc. of
   ASCE, Vol 102, No. EM2, April 1976, pp. 249-263.

5. Baber, T. T. and Wen, Y. K., "Random Vibration of Hysteretic
   Degrading Systems,: Journal of the Engineering Mechanics
   Division, ASCE Vol. 7, No. EM6, December 1981.

6. Baber, T. T. and Wen, Y. K., "Equivalent Linearization of
   Hysteretic Structures," Proceedings of the Specialty
   Conference on Probabilistic Mechanics and Structural
   Reliability, ASCE, Tucson, Arizona, January 1979.

7. Wafa, F., "Peak Response of Hysteretic Structures," Ph.D.
   Dissertation, Department of Civil Engineering, University of
   New Mexico, Albuquerque, NM, August 1981.

8. Paez, Thomas L., Ming-Liang Wang, and Ju, Frederick D.,
   "Diagnosis of Damage in SDF Structures," University of New
   Mexico Research Rep., March 1982.

9. Udwadia, F. E. and Trifunac, M. D, "Time and Amplitude
   Dependent Response of Structures," Earthquake Engineering
   and Structural Dynamics," Vol. 2, 1974, pp. 359-378.

10. Iemura, H. and Jennings, D. C., "Hysteretic Response of a
    Nine-Story Reinforced Concrete Building," Earthquake
    Engineering and Structural Dynamics, Vol. 3, 1974, pp.
    285-201.

11. Townsend, William H. and Hansen, Robert D., "Reinforced
    Concrete Connective Hysteresis Loops," Reinforced Concrete
    Structures in Seismic Zones, ACI Publication SP-53, 1974.

12. Uzumeri, S. M., "Strength and Ductility of Cast-in-Place Beam-Column Joints," Reinforced Concrete Structures in Seismic Zones, ACI Publication SP-53, 1974.

13. Wang, M. L., Paez, T. L., Ju, F. D., "Mathematical Models for Damageable Structures," The Bureau of Engineering Research, The University of New Mexico, Albuquerque, NM, February 1983.

14. Spooner, D. C. and Dougill, J. W., "A Quantitative Assessment of Damage Sustained in Concrete during Compressive Loading," Magazine of Concrete Research; Vol. 27, No. 92, September 1975, pp. 151-160.

15. Spooner, D. C., Pomeroy, C. D., and Dougill, J. W., "Damage and Energy Dissipation in Cement Pastes in Compression," Magazine of Concrete Research, Vol. 28, No. 94, March 1976, pp. 21-29.

16. Karsan, I. Demir and Jirsa, James D., "Behavior of Concrete under Compressive Loading," Journal of the Structural Division, ASCE, December 1969.

17. Wang, M. L., Paez, T. L., Ju, f. D., "Models for Damage Diagnosis in SDF STructures," Proceedings of the Symposium on The Interaction of Non-Nuclear Munitions with Structures, Colorado Springs, CO, May 1983.

18. Karel Rektorys, Editor, Survey of Applicable Mathematics, The MIT Press, Cambridge, MA, 1969.

APPENDIX A

ENERGY DISSIPATED RELATED TO CONCRETE DAMAGE

Introduction

This presentation describes and evaluates an experimental study of the strength reduction and behavior of plain concrete subjected to cyclic loading. It is recognized that concrete is damaged by application of stresses lower than the ultimate stress. The concrete fracture process begins at very low stress and is continuous.

The damage caused by loading to small stresses is slight and each subsequent loading over the same stress range produces a negligible increase in damage. However, as the loading stress is increased, more damage occurs. Stresses with peak values in the range of 40 percent to 100 percent of the ultimate stress produce considerable damage and subsequent loading over the same range cannot be neglected. In practical situations, when a severe excitation is applied to a structure, it is not uncommon for the peak stress to go beyond the 50 percent level of ultimate stress.

When loading is repeated, damage accumulates in a concrete specimen; consequently it no longer retains its original strength. This concept suggests that it might be useful to attempt a quantitative evaluation of damage occurring in concrete during the cyclic loading. The objective of this study is to demonstrate that concrete damage and strength reduction are related to energy dissipation under repeated loading.

When energy is dissipated during loading and unloading, an hysteresis loop is formed in the stress-strain curve as shown in Figure A1. The area enclosed represents the total energy dissipated during one cycle of loading. This dissipated energy may be classified into two parts, namely, damage and damping energy
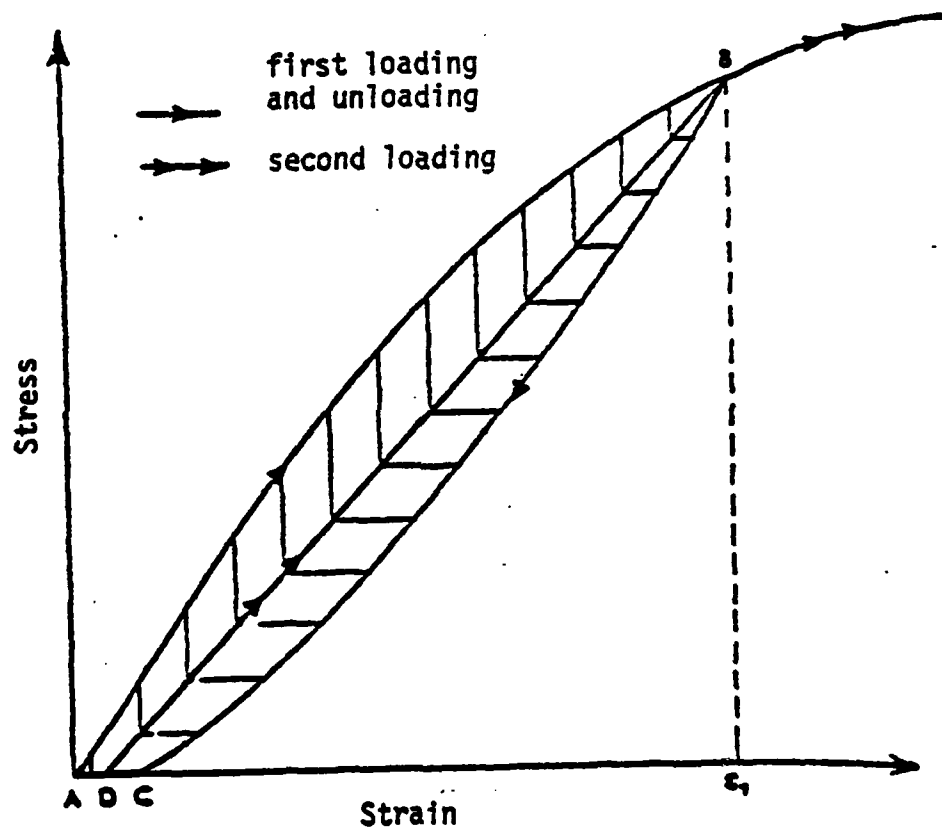
Figure A1. Idealized first and second cycles

dissipation. However, the total accumulated energy dissipation is of primary interest in this experimental study. A more detailed discussion of the energy dissipation mechanism is given in Reference [14].

There are many methods that can be used to detect and assess damage in concrete. Among the most frequently used techniques are those which assess change in initial elastic modulus, and those which measure acoustic emissions, change in pulse velocity, and energy dissipation. In the present study, the dissipated energy method will be adopted. Attention will be focused on this means for measuring damage because of its intuitive relationship with the energy dissipation of an hysteretic structure under dynamic loads. Other methods may be considered as in References [14, 15, and 16].

In the present investigation a sequence of physical experiments was performed. In each experiment a concrete cylinder (specifications given below) was loaded in uniaxial compression. The load applied to each cylinder was a cyclic load, and the energy dissipated was calculated. This was done by plotting the stress versus strain diagram and by determining the area enclosed within the hysteresis loops. Varying amounts of energy were dissipated in the various test specimens, and upon completion of cyclic testing each specimn was loaded to failure in order to determine its residual strength. For each test specimen, dissipated energy and residual strength were recorded and the relation between these quantities was established.

More details of the testing procedure are given below, together with fresh concrete properties observed during the mixing. These may provide a useful reference for the concretes used in the test.

63

The concrete specimens tested in this investigation have the mix details and plastic properties of fresh concrete as shown in Table A1.

TABLE A1.
Concrete Mix Details

Type of Cement	W/C Ratio	Aggregate Cement Ratio	Ratio of Coarse:Fine Aggregate	Maximum Aggregate Size (in)
Type 1 A	0.53	4.8	60:40	3/4

Plastic Properties of Fresh Concrete

Mix No.	Slump (in)	Air %	Room Temperature (degrees C)	Unit Weight lb/ft^3
2 WE	4	3.5	27	145.8
3 WE	4 1/4	4	30	148.96

The specimens were all cast in 6-in x 12-in steel cylinder molds. The concrete mix proportions were constant for all the specimens. The specimens were tested at a consant loading rate of 1000 lb/sec in a RIEHLE compression testing machine. The force versus strain results of each test were plotted with an x-y electronic recorder. This recorder was attached by an electronic compressometer which is properly designed for this specific purpose as shown in Figure A2. The test machine was properly calibrated before the test.

To ensure a uniform displacement of the specimens, thin sulfur caps on the two end surfaces of the specimens were employed and were allowed to harden before testing. Specimens were cured in water in the curing tank at 25°C for 14 days and 28 days.
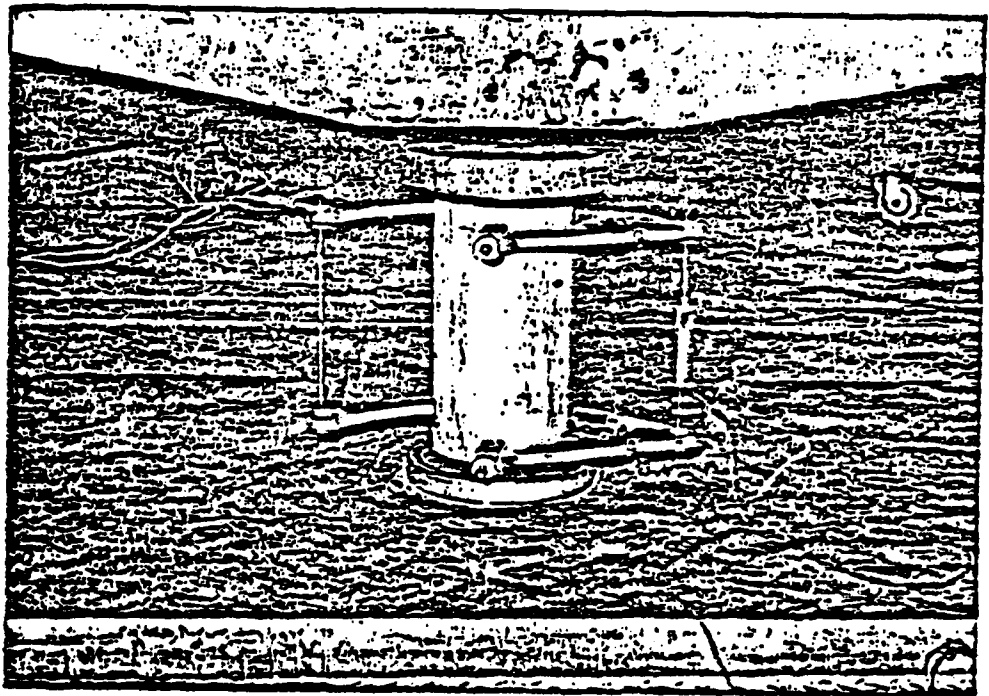
Figure A2.   Test configuration

In assessing the energy dissipated and residual strength, specimens were subjected to a series of cycles of loading and unloading. The specimens were loaded up to a value in the range of stress, 90 - 94 percent of the ultimate stress. This ensured that damage occurred for every cycle of loading. At the end of each cylce of loading and unloading, the testing machine was returned to a rest position, and reloading was commenced immediately. To ensure that concrete characteristics would be as nearly uniform as possible, all the tests in each sequence were run in one day.

Discussion of Results

Numerous physical experiments were conducted in this investigation and characteristics of concrete accumulating damage can be derived from the individual tests and all the tests, jointly. In the following section the characteristics of individual tests are discussed first; then damage characteristics related to the entire test sequence are discussed.

A typical stress-strain diagram obtained during one experiment is shown in Figure A3. A number of characteristic features can be extracted from this result. On the initial cycle the specimen was loaded to a stress near its ultimate (95 to 98 percent). It can be seen that the most significant change in behavior between consecutive loading cycles occurs between the first and second cycle.

The first loading curve shows more curvature than the following reloading curves in which curvature tends to diminish. The reloading curves show progressively decreasing slopes. This may be attributed to structural degradation of the specimen.

Another measure of degradation can be established by plotting the initial elastic modulus for a particular cycle versus energy dissipation prior to that cycle. This is shown in Figure A4. As the energy dissipated gradually increases, the initial elastic modulus diminishes.

66
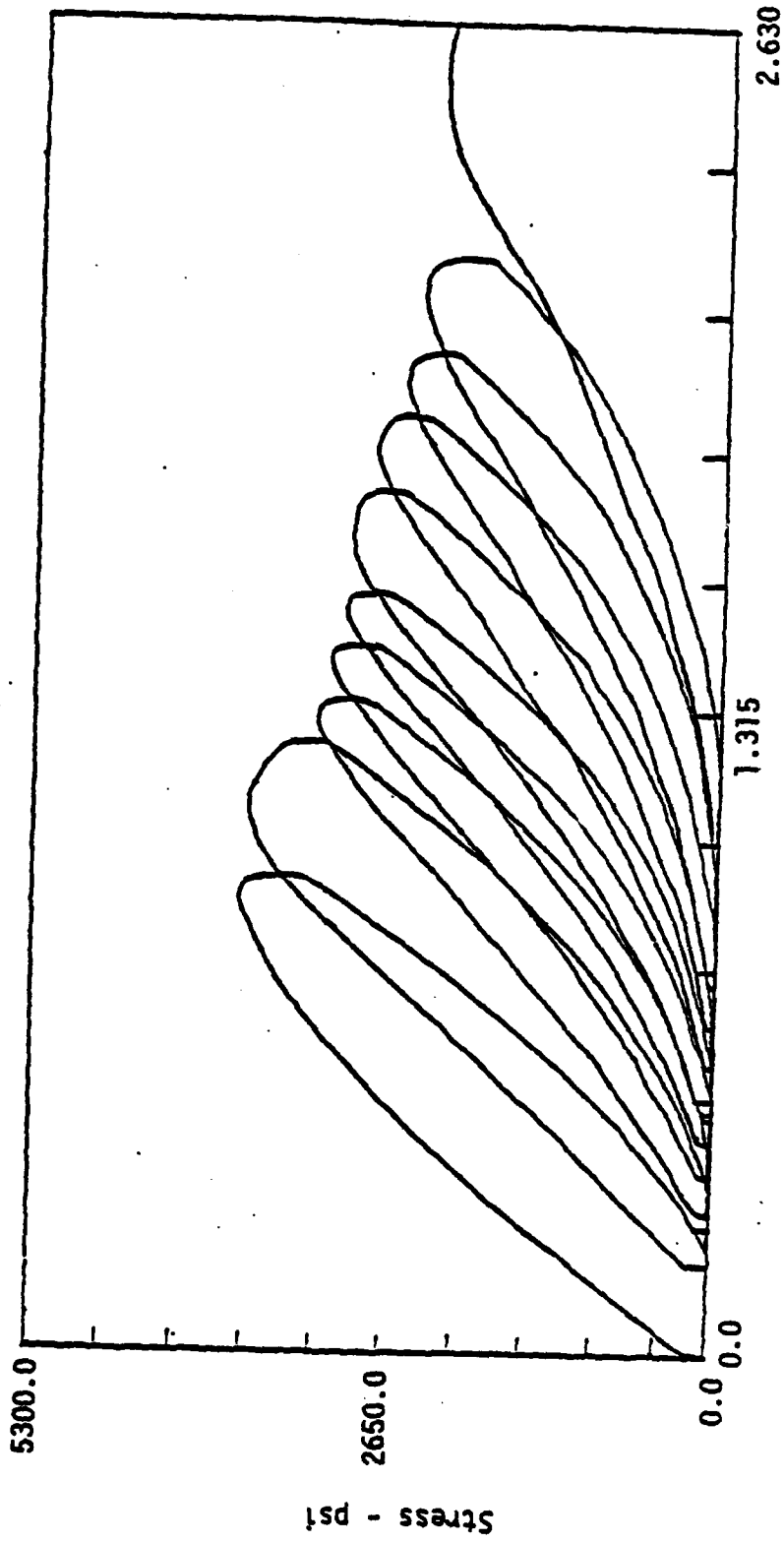
Figure A3. Stress-strain diagram for test specimen number 3WE#7
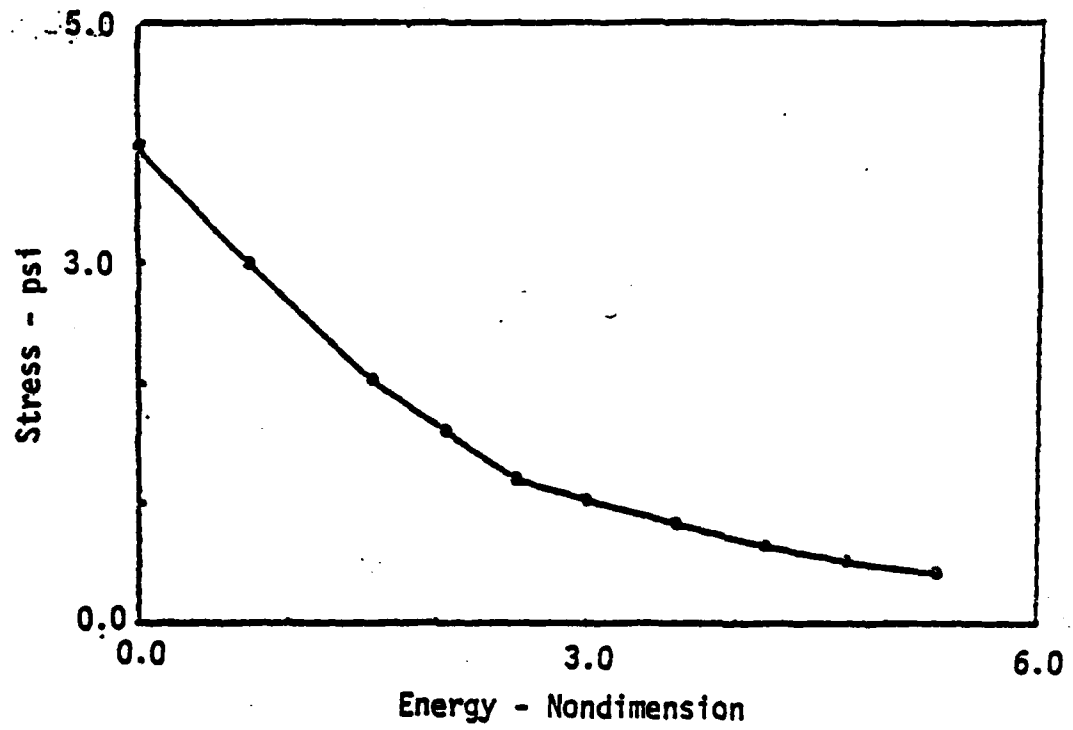
Figure A4. Initial modulus versus accumulated energy
dissipated for a typical concrete
specimen.

The above discussion was based on one typical sample. A similar discussion could be given for the other samples. Figures A5, A6, and A7 show the stress-strain curves for some other specimens tested during this investigation.

Some general characteristics of the accumulation of damage in concrete specimens can be derived from the entire collection of results. A total of 24 concrete specimens were tested in this investigation.

As noted earlier, the specimens were subjected to cyclic loadings inducing different amounts of energy dissipation in the various cylinders. Not all specimens were cycled to failure. At least, three of the specimens were tested for the determination of the ultimate strength. Other specimens, however, were cycled till failure. The remainder of the specimens were cycled till a certain amount of energy was dissipated; then these were loaded to failure in order to find their residual strength.

Using these data, a characteristic of the specimens can be extracted. The total energy dissipated by each particular specimen was plotted against the residual strength of the specimen as shown in Figure A9. Another result can be illustrated by plotting the total energy dissipated versus percentage of decrease in strength as shown in Figure A8. Both diagrams show a decrease in strength as the total energy dissipated is increased. Since only a limited number of specimens were tested, no direct mathematical expression relating the residual strength to the total energy dissipated was obtained. While such a relation could be established, further testing is required to derive a general relationship. However, the pesent results provide the information needed to conclude that energy dissipation is truly related to the residual strength.
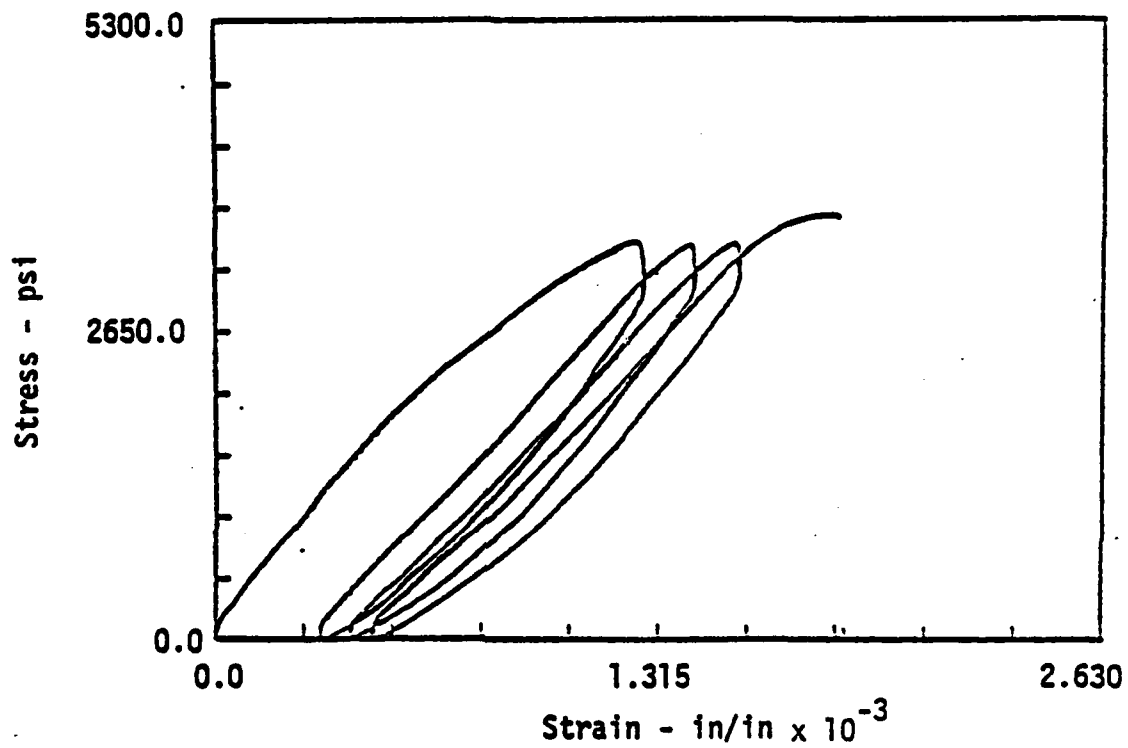
Figure A5.   Typical stress-strain diagram for a con-
crete test specimen under cyclic load.
Peak stress 90 percent of failure stress
for Batch #3 (14 days curing)

70
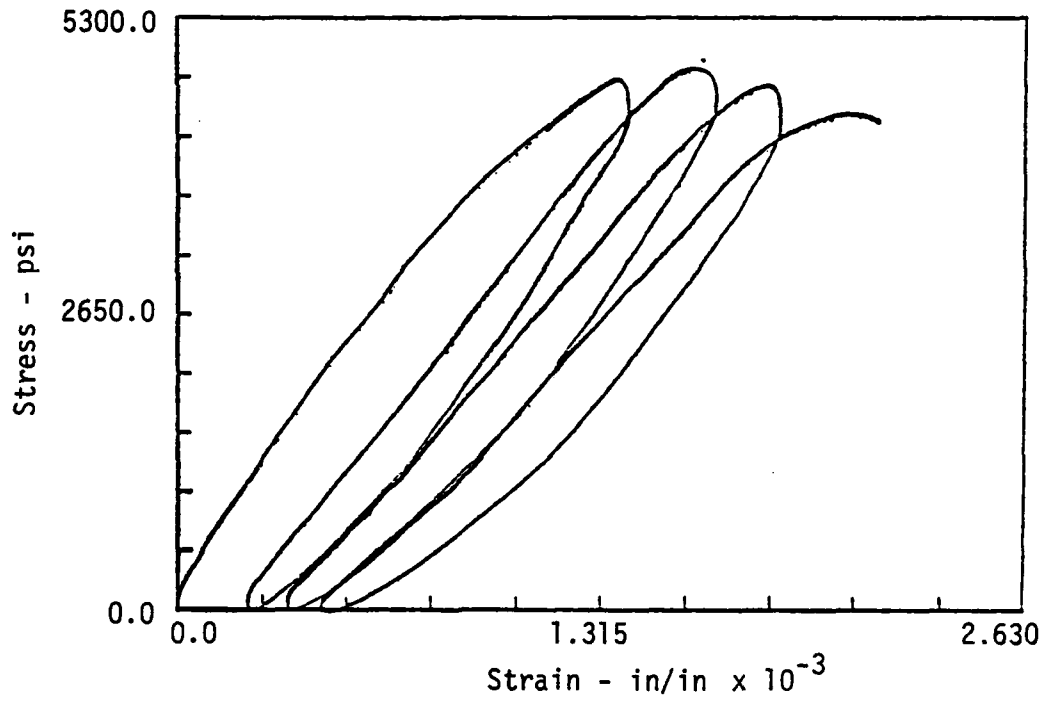
Figure A6. Typical stress-strain diagram for a
concrete test specimen under cyclic
load. Peak stress 90 percent of
failure stress for Batch #2
(28 days curing)
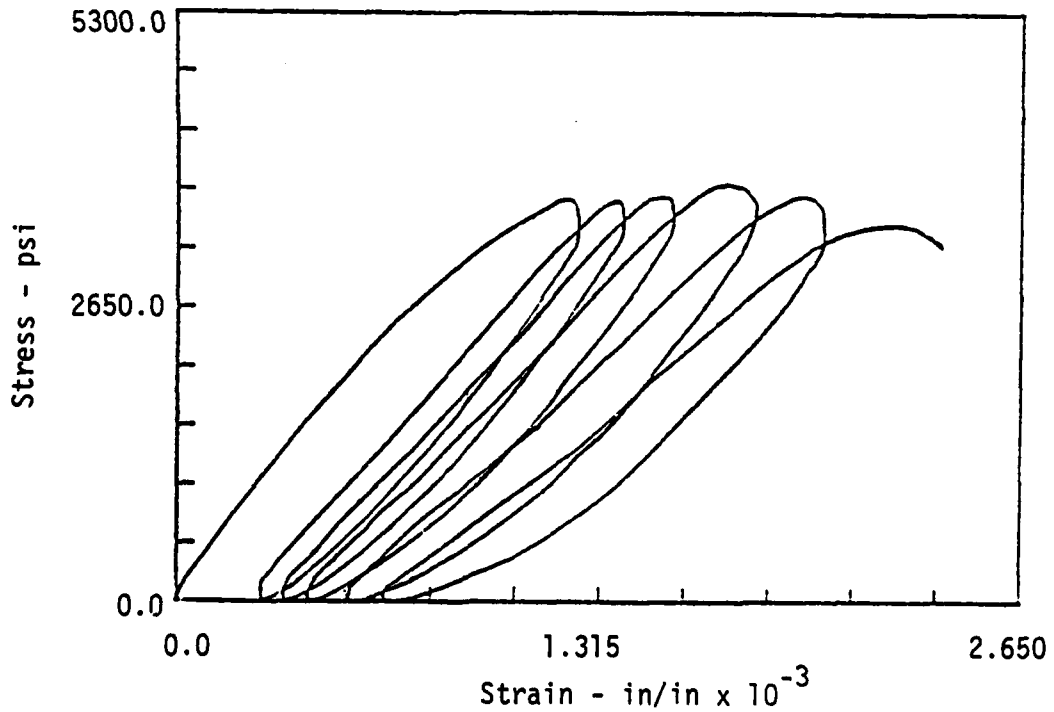
Figure A7. Typical stress-strain diagram for a
concrete test specimen under cyclic
load. Peak stress 90 percent of
failure stress for Batch #3
(14 days curing)

71
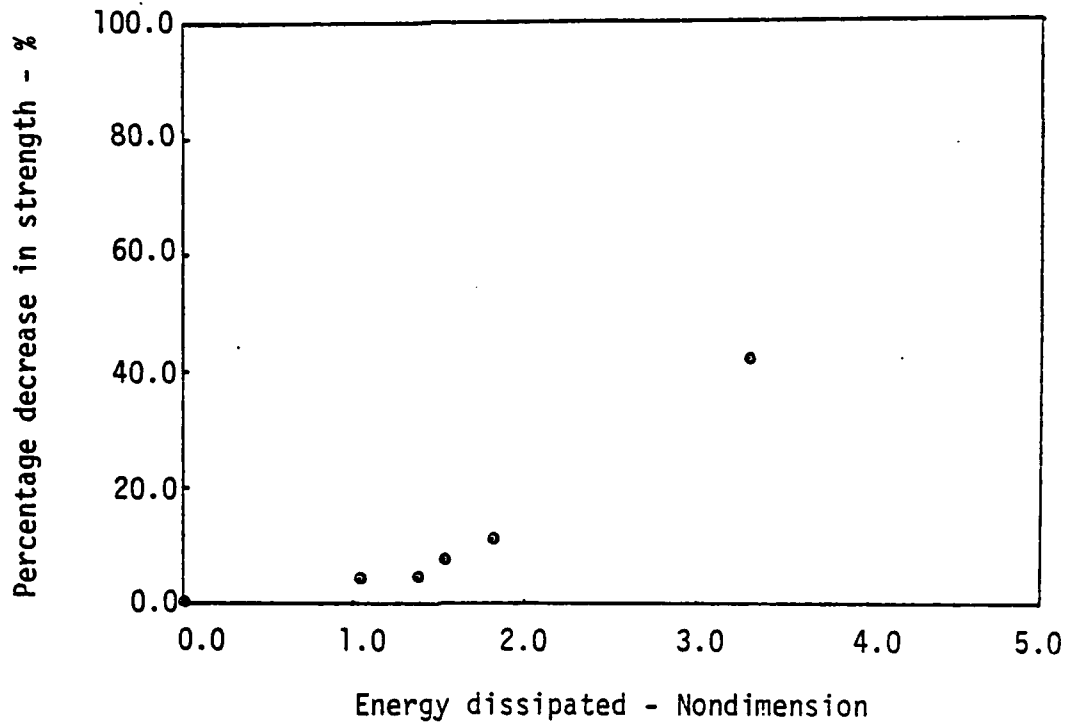
Figure A8. Percent decrease in residual strength versus energy dissipated in concrete specimen (14 day curing)
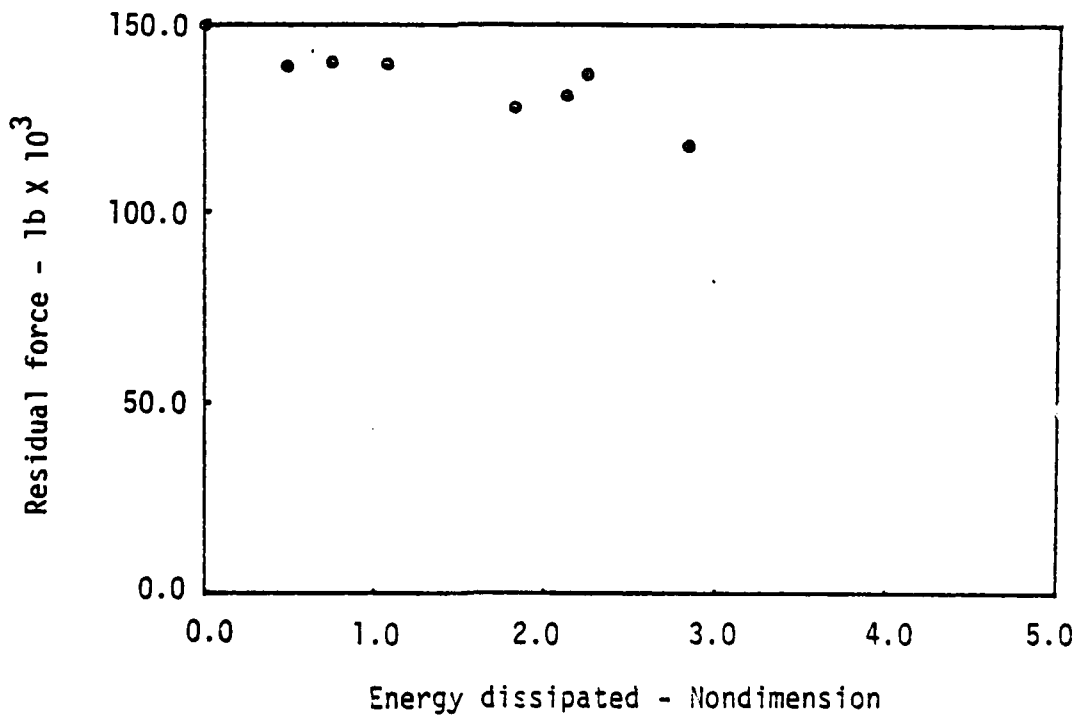
Figure A9. Residual strength versus energy dissipated in concrete specimens (28 day curing)

72

The experimental technique described above provides an approach for the estimation of damage in concrete. Based on the physical experiments, the following conclusions can be made:

1. The most significant change in the properties of the concrete occur between the first cycle and second cycle when loading in the first cycle is severe.

2. The initial elastic modulus of the specimens gradually diminishes as energy is dissipated. This implies that the damage of concrete under cyclic loading occurs progressively.

3. The energy dissipated in a concrete specimen is adversely related to residual strength. As the energy dissipated increases, the residual strength decreases. Therefore, energy dissipated may be used to predict the damage of a structure under a severe loading. Moreover, total energy dissipated may be considered as an indicator of the degree of damage in an hysteretic structure.

Some restrictions apply to the above conclusions. The work is limited to behavior in uniaxial compression. Other types of loading are possible and further tests are required to characterize damage under general loading. It has been assumed that the creep effect is small enough to be neglected in this investigation.

APPENDIX B

COMPUTER PROGRAM PUR

```
C      ***************************************
C      ***********PROGRAM NAME "PUR"***********
C      ***************************************
C      THIS PROGRAM IDENTIFIES THE PARAMETERS OF A
C      TIME VARYING SECOND-ORDER LINEAR MODEL BY
C      USING THE PERTURBATION METHOD AND ITERATIVE
C      NEWTON- RAPHSON PROCEDURE. IT MAY ALSO USE
C      THE POLYNOMIAL FITTING APPROACH.
C
       COMPLEX FF(1024),FD(1024)
       COMPLEX ZZ(1024),HD,Z(1024),HABS(512)
       DIMENSION DD(1024),F(1024),HMOD(512),HZ(512)
       DIMENSION EK(3),COE(4),S(9),INDEX(9),AS(9)
       COMMON/ARRAY/FF,FD
       CALL OPSYS('ALLOC','FD1',10)
       CALL OPSYS('ALLOC','RH1',7)
       CALL OPSYS('ALLOC','NFL',4)
       EXTERNAL MATINV
C
C      SM    : SYSTEM MASS
C      ALPHA : DAMPING COEFFICIENT
C      BETA  : STIFFNESS COEFFICIENT
C      ZETA  : DAMPING RATIO
C      C1    : INITIAL GUESS 'DAMPING'
C      C2    : INITIAL GUESS 'ALPHA*C1'
C      C3    : INITIAL GUESS 'STIFFNESS'
C      C4    : INITIAL GUESS 'BETA*C3'
C      ESLON : ACCURACY MEASURE(FOR ESLON1-ESLON4)
C      W1-W4 : ACCURACY MEASURE FOR NEWTON METHOD
C      DA1-DA4 : INCREMENT VALUES
C
       SM=1.0
       C1=1.5
       C2=0.02
       C3=37.5
       C4=-0.01
       ZETA=0.1
       ESLON1=0.02
       ESLON2=0.02
       ESLON3=0.02
       ESLON4=0.02
       WN=SQRT(C3/SM)
       DA1=0.01
       DA2=0.001
       DA3=1.0
       DA4=0.01
       W1=0.01
       W2=0.01
       W3=0.01
       W4=0.01
       PI=3.1415926535
       DT=0.05
```

74

```fortran
      M=10
      N=2**M
      NT=N/8
      TT=DT*N
      DW=2.*PI/TT
      NS=N/2
      CA=PI/NS
C
C     READ IN THE TIME DOMAIN RESPONSE
C
      READ(10,80) (F(I),DD(I),I=1,N)
C
C     WINDOW THE DATA
C
      DO 3 I=1,NS
      IM=N-I+1
      CMULT=0.5*(1.0-COS((I-1)*CA))
      F(IM)=CMULT*F(IM)
      DD(IM)=CMULT*DD(IM)
    3 CONTINUE
C
C     FFT THE INPUT AND RESPONSE
C
      DO 8 I=1,N
      FF(I)=CMPLX(F(I),0.0)*TT
      ZZ(I)=CMPLX(DD(I),0.0)*TT
    8 CONTINUE
      CALL FFT1(FF,M,N,-1.0)
      CALL FFT1(ZZ,M,N,-1.0)
C
C     FIND THE MOD(H)
C
      DO 9 I=1,NT
      FA=CABS(FF(I))
      ZA=CABS(ZZ(I))
      HMOD(I)=ZA/FA
    9 CONTINUE
C
C     CALCULATE THE DERIVATIVE OF FF
C
      DO 12 I=1,N
      TC=(I-1)*DT
      F(I)=F(I)*TC
      FD(I)=CMPLX(F(I),0.0)*TT
   12 CONTINUE
      CALL FFT1(FD,M,N,-1.)
      DO 13 I=1,N
   13 FD(I)=FD(I)*CMPLX(0.0,-1.)
C
C     FIND THE NUMBER OF PTS NEEDED IN THE BAND
C
      NC=(1.0*ZETA*WN)/DW
```

```fortran
      NW=WN/DW
      NS=NW-NC
      NF=NW+NC
      AA1=C1
      AA2=C2
      AA3=C3
      AA4=C4
   26 L=1
   28 WRITE(6,89)C1,C2,C3,C4
      ICOUNT=2
      ISTEA=ICOUNT
      AC1=C1
      AC2=C2
      AC3=C3
      AC4=C4
C
C     CALL SUBROUTINE PURT TO FIND THE MODULUS
C     OF H FROM THE MEASURED INPUT
C
   29 WN=SQRT(C3/SM)
      NC=(1.0*ZETA*WN)/DW
      NW=WN/DW
      NS=NW-NC
      NF=NW+NC
      CALL PURT(DW,NT,C1,C2,C3,C4,HZ)
C
C     FIND E(ERROR MEASURE)
C
      EE=0.0
      DO 30 I=NS,NF
      E=HMOD(I)-HZ(I)
      EE=EE+(E**2)
   30 CONTINUE
      EK(ICOUNT)=EE
      IF(ICOUNT.EQ.3) GO TO 50
      GO TO (31,32,33,34),L
   31 IF(ICOUNT.EQ.1) GO TO 40
      C1=C1-DA1
      ICOUNT=ICOUNT-1
      GO TO 29
   40 C1=AC1+DA1
      ICOUNT=ISTEA+1
      GO TO 29
   32 IF(ICOUNT.EQ.1) GO TO 41
      C2=C2-DA2
      ICOUNT=ICOUNT-1
      GO TO 29
   41 C2=AC2+DA2
      ICOUNT=ISTEA+1
      GO TO 29
   33 IF(ICOUNT.EQ.1) GO TO 42
      C3=C3-DA3
```

76

```
                    ICOUNT=ICOUNT-1
                    GO TO 29
              42    C3=AC3+DA3
                    ICOUNT=ISTEA+1
                    GO TO 29
              34    IF(ICOUNT.EQ.1) GO TO 43
                    C4=C4-DA4
                    ICOUNT=ICOUNT-1
                    GO TO 29
              43    C4=AC4+DA4
                    ICOUNT=ISTEA+1
                    GO TO 29
        C
        C           CALCULATE THE FIRST AND SECOND DERIVETIVES
        C
              50    GO TO(60,61,62,63),L
              60    TD=DA1
                    AV=AC1
                    W=W1
                    GO TO 70
              61    TD=DA2
                    AV=AC2
                    W=W2
                    GO TO 70
              62    TD=DA3
                    AV=AC3
                    W=W3
                    GO TO 70
              63    TD=DA4
                    AV=AC4
                    W=W4
                    GO TO 70
              70    DEK=(EK(3)-EK(1))/(2.0*TD)
                    DDEK=(EK(3)-2.*EK(2)+EK(1))/(TD**2)
        C
        C           DO THE NEWTON RAPHSON METHOD
        C
                    ACC=AV-(DEK/DDEK)
                    WE=ABS((ACC-AV)/ACC)
                    WD=WE-W
                    IF(WD.LE.0.0) GO TO 87
              99    GO TO(101,102,103,104),L
             101    C1=ACC
                    GO TO 28
             102    C2=ACC
                    GO TO 28
             103    C3=ACC
                    GO TO 28
             104    C4=ACC
                    GO TO 28
              87    GO TO(92,93,94,95),L
              92    C1=ACC
```

```fortran
         GO TO 85
      93 C2=ACC
         GO TO 85
      94 C3=ACC
         GO TO 85
      95 C4=ACC
      85 L=L+1
         IF(L.EQ.5) GO TO 100
         GO TO 28
C
C        COMPARE THE PARAMETERS
C
     100 CD1=ABS((AA1-C1)/C1)
         CD2=ABS((AA2-C2)/C2)
         CD3=ABS((AA3-C3)/C3)
         CD4=ABS((AA4-C4)/C4)
         IF(CD1.GT.ESLON1) GO TO 81
         IF(CD2.GT.ESLON2) GO TO 81
         IF(CD3.GT.ESLON3) GO TO 81
         IF(CD3.GT.ESLON4) GO TO 81
         WRITE(6,*) C1,C2,C3,C4
         GO TO 88
      81 AA1=C1
         AA2=C2
         AA3=C3
         AA4=C4
         GO TO 26
      80 FORMAT(2E12.4)
      82 FORMAT(3E13.4)
      89 FORMAT(4E12.4)
     150 FORMAT(2E16.6)
      88 STOP
         END
C
C        PERTURBATION METHOD
C
         SUBROUTINE PURT(DW,NT,C1,C2,C3,C4,HA)
         COMPLEX FF(1024),FD(1024),HABS(512),Z(512)
         COMPLEX HD,H,HDEV,H1,H2,H3,H4
         DIMENSION HA(NT)
         COMMON/ARRAY/FF,FD
         SM=1.0
         DO 14 I=1,NT
         W=(I-1)*DW
         HD=CMPLX((C3-SM*(W**2)),W*C1)
         H=1.0/HD
         HDEV=CMPLX((2.*SM*W),-C1)/(HD**2)
         H1=H*FF(I)
         H2=C2*H*(H1+W*(HDEV*FF(I)+H*FD(I)))
         H3=CMPLX(0.0,-C4)*H*(HDEV*FF(I)+H*FD(I))
         Z(I)=H1+H2+H3
         H4=HDEV+H*(FD(I)/FF(I))
```

78

```fortran
      HABS(I)=H*(1.0+C2*(H+W*H4)-CMPLX(0.0,C4)*H4)
      HA(I)=CABS(HABS(I))
   14 CONTINUE
      GO TO 10
   10 RETURN
      END
C
C     FFT PROGRAM
C
C     ********************************************
C     MULTIPLIED BY T WHEN USING THE FORWARD FFT
C     DIVIDED BY DT FOR BACKWARD FFT
C     SIGN =-1. FOR DFT, SIGN=1. FOR IDFT
C     ********************************************
C
      SUBROUTINE FFT1(A,N,NB,SIGN)
      COMPLEX A(NB),U,W,T
C
C     DIVIDE ALL ELEMENT BY NB
C
      DO 1 J=1,NB
    1 A(J)=A(J)/NB
C
C     REORDER SEQUENCE
C
      NBD2=NB/2
      NBM1=NB-1
      J=1
      DO  4 L=1,NBM1
      IF(L.GE.J) GO TO 2
      T=A(J)
      A(J)=A(L)
      A(L)=T
    2 K=NBD2
    3 IF(K.GE.J) GO TO 4
      J=J-K
      K=K/2
      GO TO 3
    4 J=J+K
C
C     CALCULATE FFT
C
      PI=3.141592653589793
      DO 6 M=1,N
      U=(1.0,0.0)
      ME=2**M
      K=ME/2
      W=CMPLX(COS(PI/K),SIGN*SIN(PI/K))
      DO 6 J=1,K
      DO 5 L=J,NB,ME
      LPK=L+K
      T=A(LPK)*U
```

```fortran
      A(LPK)=A(L)-T
    5 A(L)=A(L)+T
    6 U=U*W
      RETURN
      END
C
C     LEAST SQUARE POLYNOMINAL FITTING
C
C     A POLYNOMIAL FIT SUBROUTINE
C     THIS PROGRAM IS PREPARED SO THAT IT CAN
C     BE USED WHENEVER IT IS NECESSARY.
C
      SUBROUTINE FIT(Y,MP,N,X1,X2,A)
      DIMENSION XX(9,4),Y(9),X(9),XP(4,4),A(4),D(4,4),B(4)
      DIMENSION EPS(9)
      DX=(X2-X1)/FLOAT(N-1)
      DO 10 I=1,N
   10 X(I)=X1+FLOAT(I-1)*DX
      DO 1 I=1,N
      XX(I,1)=1.0
      DO 1 J=2,MP
    1 XX(I,J)=X(I)**(J-1)
      DO 2 I=1,MP
      DO 2 J=I,MP
      XP(I,J)=0.0
      DO 2 K=1,N
    2 XP(I,J)=XP(I,J)+XX(K,I)*XX(K,J)
      DO 3 I=2,MP
      IM=I-1
      DO 3 J=1,IM
    3 XP(I,J)=XP(J,I)
      CALL MATINV(XP,MP,D)
      DO 4 I=1,MP
      B(I)=0.0
      DO 4 J=1,N
    4 B(I)=B(I)+XX(J,I)*Y(J)
      DO 5 I=1,MP
      A(I)=0.0
      DO 5 J=1,MP
    5 A(I)=A(I)+D(I,J)*B(J)
      RETURN
      END
C
C     MATRIX INVERSION
C
      SUBROUTINE MATINV(C,N,D)
C     MATRIX INVERSION C-INPUT  D-OUTPUT
      DIMENSION C(4,4),D(4,4)
      DO 10 J=1,N
      DO 10 K=1,N
   10 D(J,K)=0.0
      DO 11 K=1,N
```

```
   11 D(K,K)=1.0
      P1=1.0
      DO 55 I=1,N
      P2=C(I,I)
      DO 40 J=1,N
      C(I,J)=C(I,J)/P2
   40 D(I,J)=D(I,J)/P2
      DO 51 IC=1,N
      P3=-C(IC,I)
      DO 50 K=1,N
      IF(IC-I)21,51,21
   21 C(IC,K)=C(I,K)*P3+C(IC,K)
   50 D(IC,K)=D(I,K)*P3+D(IC,K)
   51 CONTINUE
      P1=P2*P1
      IF((I+2)-N)55,53,55
   53 DET=P1*((C(I+1,I+1)*C(I+2,I+2))
     *-(C(I+2,I+1)*C(I+1,I+2)))
   55 CONTINUE
      DO 70 IT=1,N
      DO 70 IS=1,N
   70 C(IT,IS)=D(IT,IS)
      RETURN
      END
```

END

FILMED

1-84

DTIC